

## **Ex vivo activation of pyruvate kinase improves red blood cell metabolism and hydration in hereditary spherocytosis.**

Tracking no: RCI-2024-000102R1

Jonathan de Wilde (University Medical Center Utrecht, Netherlands) Titine Ruitter (University Medical Center Utrecht, Netherlands) Jennifer Bos (University Medical Center Utrecht, Utrecht University, Netherlands) Marissa Traets (University Medical Center Utrecht, Netherlands) Brigitte van Oirschot (University medical Center, Netherlands) Thomas Doeven (University Medical Center Utrecht, Netherlands) Judith Jans (University Medical Center Utrecht, Netherlands) Megan Wind-Rotolo (Agiros Pharmaceuticals, Inc., United States) Andreas Glensthøj (Danish Red Blood Cell Center, Department of Hematology, Copenhagen University Hospital - Rigshospitalet, Denmark) Wouter van Solinge (UMC Utrecht, Netherlands) Eduard van Beers (University Medical Center Utrecht, Netherlands) Marije Bartels (University Medical Centre Utrecht, Netherlands) Minke Rab (University Medical Center Utrecht, Netherlands) Richard van Wijk (University Medical Center Utrecht, Netherlands)

### **Abstract:**

Hereditary spherocytosis (HS) is a hereditary hemolytic anemia with limited treatment options. A relative decrease in activity of pyruvate kinase (PK), an essential glycolytic enzyme in red blood cells, has been described in patients with HS. Due to their dependence on glycolysis, PK activation therapy could therefore potentially improve red cell health in HS. The aim of this study was to evaluate PK activity in HS red blood cells, and to investigate the effect of two PK activators (mitapivat and tebapivat). Blood samples from eighteen non-transfusion-dependent HS patients (splenectomized and non-splenectomized) were analyzed. Our results confirmed impaired glycolysis in HS at baseline, indicated by a relatively decreased PK activity (PK to hexokinase ratio: 7.6 in HS vs. 11.4 in controls). PK activity (increase >50%) and ATP levels (increase >44%) improved upon ex vivo treatment with mitapivat and tebapivat. Metabolomics showed various metabolic alterations upon treatment. Furthermore, the hydration state of the cells improved (Ohyper increase >2.1%). No improvements were found in deformability, intracellular calcium and cellular adhesion to laminin. When comparing splenectomized patients to non-splenectomized patients, we found that PK thermostability in non-splenectomized patients was decreased more than in splenectomized patients. Following this, PK activator therapy improved PK thermostability to a greater extent in red blood cells from splenectomized patients, which appears to relate to the degree of reticulocytosis. Overall, we demonstrated that PK activation improves the metabolic and cellular properties of HS red blood cells ex vivo, supporting the rationale for further evaluation of PK activation in HS.

**Conflict of interest:** COI declared - see note

**COI notes:** DISCLOSURE OF CONFLICTS OF INTEREST: JdW, JB, MT, AG, EvB, MR and RvW receive research funding from Agios Pharmaceuticals Inc. EvB, MR and RvW are consultants for Agios Pharmaceuticals Inc. MW-R is a current employee of Agios Pharmaceuticals Inc. AG receives research funding from Agios, Bristol Myers Squibb, Saniona, and Sanofi and has done consulting for Agios, Bristol Myers Squibb, Novo Nordisk, Pharmacosmos, and Vertex Pharmaceuticals. MR and RvW have received research funding from Axcella Health and RR Mechatronics. RvW has done consulting for Pfizer.

**Preprint server:** No;

**Author contributions and disclosures:** AUTHORSHIP CONTRIBUTIONS: MR and RvW designed and supervised the project, as well as acquired the funding for the project. JdW coordinated the project. JdW, TR, JB, MT and BvO performed experiments and collected data. JdW, TD, MT, EvB, MB and MR recruited patients and acquired patient data. JdW and TR performed the data analysis. JdW, MR and RvW wrote the original draft. All authors reviewed and edited the manuscript.

**Non-author contributions and disclosures:** No;

**Agreement to Share Publication-Related Data and Data Sharing Statement:** DATA AVAILABILITY STATEMENT: Data and protocols are available upon request (e-mail r.vanwijk@umcutrecht). Data will be shared as is compliant with the General Data Protection Regulation and European Union privacy laws.

**Clinical trial registration information (if any):**

**TITLE:** *Ex vivo* activation of pyruvate kinase improves red blood cell metabolism and hydration in hereditary spherocytosis.

**SHORT TITLE:** Pyruvate kinase activation in spherocytosis.

**AUTHORS:** Jonathan R.A. de Wilde<sup>1</sup>, Titine J.J. Ruiter<sup>1,2</sup>, Jennifer Bos<sup>1</sup>, Marissa J.M. Traets<sup>1</sup>, Brigitte A. van Oirschot<sup>1</sup>, Thomas Doeven<sup>3</sup>, Judith J.M. Jans<sup>2</sup>, Megan Wind-Rotolo<sup>4</sup>, Andreas Glenthøj<sup>5,6</sup>, Wouter W. van Solinge<sup>1</sup>, Eduard J. van Beers<sup>3</sup>, Marije Bartels<sup>3</sup>, Minke A.E. Rab<sup>1,7</sup> and Richard van Wijk<sup>1</sup>.

**AFFILIATIONS:**

<sup>1</sup>Red Blood Cell Research Group, Central Diagnostic Laboratory-Research, University Medical Center Utrecht, Utrecht University, Utrecht, the Netherlands, <sup>2</sup>Section Metabolic Diagnostics, Department of Genetics, University Medical Center Utrecht, Utrecht University, Utrecht, the Netherlands, <sup>3</sup>Center for Benign Hematology, Thrombosis and Hemostasis, Van Creveldkliniek, University Medical Center Utrecht, Utrecht University, Utrecht, The Netherlands, <sup>4</sup>Agios Pharmaceuticals, Inc., Cambridge, Massachusetts, United States of America, <sup>5</sup>Danish Red Blood Center, Department of Hematology, Copenhagen University Hospital – Rigshospitalet, Copenhagen, Denmark, <sup>6</sup>Department of Clinical Medicine, University of Copenhagen, Copenhagen, Denmark, <sup>7</sup>Department of Hematology, Erasmus Medical Center Rotterdam, the Netherlands.

**CORRESPONDENCE:**

Dr. Richard van Wijk, Central Diagnostic Laboratory - Research, University Medical Center Utrecht, Utrecht University, Heidelberglaan 100, 3584 CX, Utrecht, The Netherlands. E-mail: [r.vanwijk@umcutrecht.nl](mailto:r.vanwijk@umcutrecht.nl)

**WORD COUNT:**

Abstract: 249

Main text: 4069

Figures: 5

Tables: 1

References: 69

Supplemental material: supplemental methods, 8 supplemental figures, 2 supplemental data files

**SCIENTIFIC CATEGORY:**

Red Cells, Iron, and Erythropoiesis

**KEY POINTS:**

- The activity of the key glycolytic enzyme pyruvate kinase is relatively decreased in hereditary spherocytosis red blood cells
- *Ex vivo* treatment with pyruvate kinase activators lead to increased ATP levels and an improved hydration state

**ABSTRACT:**

Hereditary spherocytosis (HS) is a hereditary hemolytic anemia with limited treatment options. A relative decrease in activity of pyruvate kinase (PK), an essential glycolytic enzyme in red blood cells, has been described in patients with HS. Due to their dependence on glycolysis, PK activation therapy could therefore potentially improve red cell health in HS. The aim of this study was to evaluate PK activity in HS red blood cells, and to investigate the effect of two PK activators (mitapivat and tebapivat). Blood samples from eighteen non-transfusion-dependent HS patients (splenectomized and non-splenectomized) were analyzed. Our results confirmed impaired glycolysis in HS at baseline, indicated by a relatively decreased PK activity (PK to hexokinase ratio: 7.6 in HS vs. 11.4 in controls). PK activity (increase >50%) and ATP levels (increase >44%) improved upon *ex vivo* treatment with mitapivat and tebapivat. Metabolomics showed various metabolic alterations upon treatment. Furthermore, the hydration state of the cells improved ( $O_{\text{hyper}}$  increase >2.1%). No improvements were found in deformability, intracellular calcium and cellular adhesion to laminin. When comparing splenectomized patients to non-splenectomized patients, we found that PK thermostability in non-splenectomized patients was decreased more than in splenectomized patients. Following this, PK activator therapy improved PK thermostability to a greater extent in red blood cells from splenectomized patients, which appears to relate to the degree of reticulocytosis. Overall, we demonstrated that PK activation improves the metabolic and cellular properties of HS red blood cells *ex vivo*, supporting the rationale for further evaluation of PK activation in HS.

## INTRODUCTION:

Hereditary spherocytosis (HS) is a hereditary hemolytic anemia caused by pathogenic variants in genes encoding for various red blood cell (RBC) membrane and cytoskeletal proteins. Due to a decrease in synthesis or dysfunction of these proteins, the membrane becomes unstable, leading to weakened anchoring of the lipid bilayer to the cytoskeleton.<sup>1</sup> This weakening causes membrane loss through vesiculation, a subsequent reduced surface-to-volume ratio, and ultimately, the spherocytic shape of the RBC. These less deformable spherocytes become entrapped in the splenic environment, leading to hemolytic anemia.<sup>2</sup> The five major proteins involved in HS are alpha-spectrin (*SPTA1*, OMIM #270970), beta-spectrin (*SPTB*, OMIM #616649), ankyrin-1 (*ANK1*, OMIM #182900), band 3 (also known as anion exchanger 1) (*SLC4A1*, OMIM #612653) and protein 4.2 (*EPB42*, OMIM #612690). HS patients suffer from a variable degree of anemia, which complicates clinical decision-making.<sup>3</sup> Splenectomy is common but is accompanied by susceptibility to encapsulated bacteria and increased risk of thrombosis.<sup>3</sup> In children, splenectomy is preferably postponed until age >5 years to facilitate maturation of the immune system. In severely affected children, partial splenectomy may be considered, yielding similar improvements in hemoglobin levels whilst possibly having a lower risk for infections<sup>4,5</sup>. Ultimately, RBC transfusions may be required. Altogether, there is a need for novel, less-invasive, treatment options in HS.

Pyruvate kinase (PK) activation has been studied as a potential therapeutic option in rare anemias.<sup>6-13</sup> Initially focused on PK deficiency (PKD), the allosteric activation of the key glycolytic enzyme PK via small molecules was hypothesized to have beneficial effects in other RBC disorders.<sup>14</sup> Activation of wild-type PK *ex vivo* in several disorders has shown to increase ATP levels.<sup>15,16</sup> In clinical studies where patients with sickle cell disease (SCD) and both non-transfusion- and transfusion-dependent thalassemia were treated with the PK activator mitapivat, hemoglobin levels increased.<sup>7-11</sup> Interestingly, a recent study by Matte et al. demonstrated that, in a protein 4.2-deficient mouse model of HS, mitapivat treatment decreased hemolysis and was not inferior to splenectomy.<sup>17</sup>

Several studies suggested decreased PK activity and glycolytic flux in HS.<sup>17-19</sup> As ATP is needed to ensure proper RBC deformability and hydration, disturbed glycolysis may hamper the function and survival of already compromised RBCs.<sup>2</sup> Andres et al. observed a decrease in PK activity in RBCs of HS patients.<sup>19</sup> It was hypothesized that membrane instability in HS leads to loss of complexes of glycolytic enzymes residing in the RBC membrane. The loss of these complexes, which include PK, would then reduce local availability of PK.<sup>19-21</sup> However, as decreased PK activity is a feature of various hereditary hemolytic anemias, it cannot be excluded that other factors contribute to this relatively decreased activity of PK.<sup>14</sup>

Recently, a phase 2 clinical trial in which adult patients with HS are treated with mitapivat has started (NCT05935202).<sup>22,23</sup> However, to date, no *ex vivo* studies have investigated the detailed effect of PK activators on RBC characteristics in humans with HS. Here we characterized PK in detail in RBCs derived from patients with HS. We found that PK activity was relatively decreased. Upon *ex vivo* PK activation, glycolysis was enhanced with subsequent beneficial effects on RBC hydration. Therefore, our findings support the rationale for further evaluation of PK activation in HS.

## **MATERIALS AND METHODS:**

The methods are briefly described below. A detailed description of the methods, including statistical analysis, can be found in the supplemental material.

### **Patient selection**

Patients ( $\geq 16$  years old) diagnosed with HS who were non-transfusion-dependent (no regular transfusions and no transfusion  $< 90$  days prior to blood draw) were eligible for inclusion. HS diagnosis was established via our in-house RBC disorders diagnostic routine, which includes osmotic gradient ektacytometry, eosin-5-maleimide (EMA) binding test, and a targeted next-generation sequencing gene panel. Disease severity was determined based on both hemoglobin values and reticulocyte percentage<sup>3,24</sup>. Blood was collected via venipuncture in either EDTA (for hematological indices of untreated whole blood) or lithium-heparin tubes (for hematological indices of *ex vivo* treated samples and for all assays performed with untreated whole blood or with *ex vivo* treated samples). This study was approved by the ethical committee of the University Medical Center Utrecht (NedMec, protocol number 21/793), according to the principles described in the declaration of Helsinki. Blood from healthy controls (HC) was collected through the University Medical Center Utrecht's minidonor service (NedMec, protocol number 18/774) and were age and ethnically matched. No male HC were available. The number of HC varied per assay and is stated within the results.

### **Hematological indices**

Whole blood, purified RBCs and *ex vivo* treated samples were analyzed by the Cell-Dyn Sapphire (Abbot Diagnostics) for routine hematological parameters. Percentage of hypochromic cells (mean corpuscular hemoglobin concentration (MCHC)  $< 28$  g/dL) and percentage of dense cells (MCHC  $> 41$  g/dL) were measured with the Advia 120/2120 hematology analyzer (Siemens Healthcare Diagnostics).

### **Purification of red blood cells**

Purification of RBCs from whole blood was performed as previously described.<sup>25</sup> RBCs were separated from white blood cells (WBCs) and platelets by filtering the whole blood over a cellulose column, after which remaining platelets are washed away.

### ***Ex vivo* treatment with pyruvate kinase activators**

Purified RBCs were diluted in buffer (containing 10 mM phosphate buffered saline, 1.2 mM adenine, 30 mM D-mannitol and 1% D-(+)-glucose solution (all Sigma-Aldrich), pH 7.40) with a final RBC concentration of  $0.08-0.1 \times 10^{12}$  RBCs/L. RBCs were then incubated with dimethylsulfoxide (DMSO, 0.1% final, Sigma-Aldrich) as vehicle control or with 10  $\mu$ M final concentration mitapivat (also known as AG-348, which was previously used at 10  $\mu$ M final concentration in *ex vivo* experiments with PKD RBCs) or 10 or 2  $\mu$ M final concentration of tebapivat (also known as AG-946) (both Agios Pharmaceuticals Inc.).<sup>26,27</sup> After incubation for 16 hours at 37 °C whilst tumbling, the cell suspension was directly used for measurement of enzyme activity. For other assays, RBCs were first concentrated in buffer (to a concentration of  $\pm 3.6 \times 10^{12}$  RBCs per liter) by centrifugation (350G for 5 minutes) and removal of buffer volume. To assess effect on PK thermostability, a different incubation method was used (described in supplemental methods).

### **Pyruvate kinase activity, thermostability and quantification**

PK enzyme activity and thermostability assays were performed according to the method of Beutler and Blume et al., respectively.<sup>25,28</sup> Activity of PK and hexokinase (HK), as well as PK activity within the PK thermostability assay (expressed as PK thermostability in percentages), was measured using a spectrophotometer (Spectramax ID3, Molecular Devices). PKR and PKM2 were quantified by western blot as described previously.<sup>29,30</sup>

### **Measurements of adenosine triphosphate and 2,3-diphosphoglycerate**

Quantitative analysis of ATP and 2,3-DPG was performed as previously described.<sup>31</sup> Metabolites were extracted from frozen stored samples (untreated whole blood or *ex vivo* treated RBCs) and measured with liquid chromatography coupled with high-resolution mass spectrometry (LC-MS/HRMS). Mass peaks were integrated and quantified based on internal standard and calibration samples using TraceFinder software.

### **Untargeted metabolomics**

For untargeted analysis of metabolites, untreated whole blood or *ex vivo* treated RBCs were spotted on a filter paper (Whatman Grade F-12) and dried for 4 hours before storage at -80 °C. Metabolites were extracted from these dried blood spots and measured with direct-infusion high-resolution mass spectrometry (DI-HRMS) as previously described.<sup>32-34</sup> A customized bioinformatics pipeline (in R programming software) was used for metabolite annotation of mean peak intensities, based on the human metabolome database.

### **Hemoglobin-oxygen affinity**

Affinity of hemoglobin for oxygen at 37 °C was assessed via the Hemox Analyzer (TCS Scientific Corporation).<sup>35</sup>

### **Ektacytometry**

RBC deformability was assessed via ektacytometry, performed on the laser optical rotational red cell analyzer (Lorcca, RR Mechatronics) as previously described.<sup>36,37</sup> Assays included osmotic gradient ektacytometry (determining deformability under an osmotic gradient), deformability assay (determining maximum deformability at different shear stresses with a range of 0.3-100 Pa) and cell membrane stability test (CMST, determining maximum deformability before and after a predefined period of shear stress (100 Pa), thereby assessing RBC membrane health).<sup>37</sup>

### **Adhesion to laminin**

*Ex vivo* treated RBCs were brought under flow through a laminin-coated (BioLamina) microfluidic slide (Ibidi) for 10 minutes at room temperature. After washing away non-adherent cells, the number of adhered RBCs were counted using the Zeiss Observer Z1 microscope (20x objective).<sup>38,39</sup>

### **Intracellular calcium quantification**

To determine intracellular calcium concentration within RBCs, we used Fluo-4-AM (Invitrogen by Thermo Fisher Scientific) and measured mean fluorescent intensity in the FITC channel by flow cytometry (FACS Canto II, BD Biosciences).

**Statistical analysis**

Data were analyzed via GraphPad Prism and MetaboAnalyst (for untargeted metabolomics). Data were adjusted to rescale the outcomes of *ex vivo* treated samples relative to vehicle (set at 100%) when appropriate. Outcomes are presented with mean±standard deviation unless stated differently. All outcomes with a *p*-value <0.05 were considered significant.

## RESULTS:

### Patient characteristics

Our cohort consisted of blood samples from 18 HS patients, originating from eleven unique families (**Table 1**). Most patients were female (12 (66.7%) vs. 6 males 33.3%) and median age was 41 (range 24-68 years). Splenectomy was performed in 7 out of 18 patients (38.9%). The median hemoglobin (Hb) in males was 15.5 g/dL (range 10.5-17.6) and in females 12.1 g/dL (8.1-15.6). Most patients did not suffer from anemia (10 patients non-anemic, 55.6%, cut-off for males 13.9 g/dL and for females 11.9 g/dL). The eight anemic patients were not splenectomized. Notably, all but one patient had reticulocytosis (reticulocyte percentage >2.5%).

### Properties of pyruvate kinase and related metabolites

PK activity in untreated RBCs was increased compared to healthy controls (HC, N=12) (mean HC  $7.3 \pm 1.7$  U/gHb vs. HS  $9.6 \pm 3.6$  U/gHb,  $p < 0.05$ ; **Figure 1A,B**). As PK is an age-dependent enzyme, we assessed whether PK activity would remain increased when correcting for RBC age. Therefore, we compared PK activity with HK, another age-dependent glycolytic enzyme.<sup>40,41</sup> PK/HK ratio was decreased (HC  $11.4 \pm 2.0$  vs. HS  $7.6 \pm 1.3$ ,  $p < 0.0001$ ; **Figure 1C,D**). Although we observed large individual variability, this demonstrates that PK activity in HS is relatively decreased. Mean PK thermostability tended to be decreased, yet this was not significant (HC (N=6)  $78.6 \pm 3.7\%$  vs. HS  $69.8 \pm 11.6\%$ ,  $p = 0.085$ ; **Figure 1E,F**). Western blot analysis was performed to determine if the decrease in activity was associated with decreased levels of PKR protein. In contrast, HS patients showed higher PKR levels than HC, likely related to reticulocytosis, as we found a correlation between PKR/Actin ratio and reticulocyte percentage (**Supplemental Figure 1A-C**). This is in line with reticulocytes having increased protein content.<sup>42</sup> No PKM2 was detected in HS RBCs (**Supplemental Figure 1D**).

Following our observation that PK activity is relatively decreased in HS, we determined the concentrations of adenosine triphosphate (ATP) and 2,3-diphosphoglycerate (2,3-DPG), both regulated by PK. In untreated whole blood, we observed no differences in ATP or 2,3-DPG between HS and HC, which also resulted in similar ATP/2,3-DPG ratios (ATP/2,3-DPG ratio in HC  $0.36 \pm 0.07$  versus  $0.43 \pm 0.09$ , not significant (ns); **Figure 1G,H**). Next, we measured hemoglobin-oxygen affinity, an important indicator for tissue-oxygen delivery. Oxygen affinity is strongly regulated by 2,3-DPG levels and is decreased in other hemolytic anemias (e.g., PKD, SCD).<sup>43,44</sup> In line with normal 2,3-DPG levels, we found that p50 values in untreated HS RBCs are similar to HC (HS  $24.1 \pm 1.7$  mmHg vs.  $25.0 \pm 1.3$  mmHg). We also observed a strong correlation between p50 and 2,3-DPG concentration ( $r = 0.835$ ,  $p < 0.0001$ ), confirming the relation of 2,3-DPG with hemoglobin-oxygen affinity (**Supplemental Figure 2**).

### Ex vivo treatment with pyruvate kinase activators enhances glycolysis

When the substrate of PK, phosphoenolpyruvate (PEP), is abundant, PK is maximally active as PEP itself is an allosteric activator of PK. Thus, when PEP is abundant, there would be no additional effect of mitapivat and tebapivat (both also allosterically activating the enzyme). Therefore, we focused on changes in PK activity at suboptimal substrate concentrations (PEP 0.5 mM final concentration). We found that mitapivat 10  $\mu$ M as well as both concentrations of tebapivat increased PK activity in all patients (N=18)

when compared to vehicle (mitapivat 10  $\mu$ M 50.8 $\pm$ 28.6% mean increase; tebapivat 10  $\mu$ M 65.3 $\pm$ 35.7%; tebapivat 2  $\mu$ M 61.3 $\pm$ 33.2%, all  $p$ <0.0001; **Figure 2A**). Increases in PK/HK ratio were similar (mitapivat 10  $\mu$ M 55.4 $\pm$ 30.5%; tebapivat 10  $\mu$ M 64.6 $\pm$ 34.2%; tebapivat 2  $\mu$ M 63.9 $\pm$ 32.2%, all  $p$ <0.0001; **Figure 2B**). Whereas PK thermostability did not differ significantly between untreated HS RBCs and HC, tebapivat stabilized PK thermostability (N=17), leading it to retain >85% of its activity (vehicle PK thermostability at T=60 minutes 37.6 $\pm$ 10.8%; mitapivat 2  $\mu$ M 46.5 $\pm$ 19.6%,  $p$ =0.17; tebapivat 2  $\mu$ M 85.7 $\pm$ 12.2%,  $p$ <0.0001; tebapivat 500 nM 85.4 $\pm$ 11.9%,  $p$ <0.0001; **Figure 2C**). In contrast, mitapivat did not induce a significant increase in thermostability. However, thermostability of lysates treated with mitapivat was still increased (when compared to vehicle) at T=20 minutes, yet showed a marked decrease at T=40 minutes (**Figure 2D**; **Supplemental Figure 3**), possibly indicating that mitapivat was unable to sustain its initial improving effect on PK thermostability in this *ex vivo* system.

Upon *ex vivo* treatment, ATP levels increased, whilst 2,3-DPG levels decreased (**Figure 2E,F**). Consequently, ATP/2,3-DPG ratio increases were nearly 5-fold (mitapivat 10  $\mu$ M 364.5 $\pm$ 193.5%; tebapivat 10  $\mu$ M 338.8 $\pm$ 91.4%; tebapivat 2  $\mu$ M 361.1 $\pm$ 166.7%, all  $p$ <0.0001) (**Figure 2G**). These data suggest that *ex vivo* PK activation in HS RBCs enhances glycolysis and subsequently provides additional ATP to RBCs.

### **Activation of pyruvate kinase affects multiple metabolic pathways**

Untargeted metabolomics of untreated HS whole blood showed various changes compared to HC (**Supplemental Figure 4, Supplemental File 1**), which were similar to those described before.<sup>18</sup> To explore the effects of *ex vivo* PK activation on the RBC metabolome of HS patients, we analyzed RBCs treated with vehicle or 2  $\mu$ M tebapivat (N=15). The dataset comprised Z-scores of 1897 unique metabolites corresponding to 3948 metabolite annotations. Principal component analysis showed close clustering of individuals without clear separation of groups, indicating only slight changes in metabolome upon *ex vivo* treatment (**Figure 3A**). *Ex vivo* treatment with tebapivat significantly changed 104/1897 metabolites as identified by paired t-tests (unadjusted  $p$ <0.05), although no metabolite reached a false discovery rate-adjusted  $p$ <0.05 (**Supplemental File 2**). Of these 104 metabolites, 68 significantly decreased and 36 significantly increased (fold-change>2.0) (**Figure 3B, Supplemental File 2**). Several glycolytic metabolites, including hexose-6-phosphate, phosphoglycerate, and PEP were significantly decreased, as expected upon PK activation. Also, the pentose phosphate pathway (PPP) metabolite 6-phosphogluconate was significantly decreased, possibly indicating that PK activation treatment could reduce the flux through the PPP. Furthermore, we observed a significant increase in inosine monophosphate (IMP), which is formed by deamination of adenosine monophosphate (AMP). Lastly, changes in fatty acid components (including glycerophospholipids, diglycerides and ceramides) were observed upon treatment with tebapivat, which could implicate an effect of PK activation on lipid metabolism and possibly the lipid bilayer. The top 50 significantly different metabolites are shown in **Figure 3C**.

### **Increased pyruvate kinase activity leads to changes in various red blood cell characteristics**

We found that mitapivat and both concentrations of tebapivat decrease p50, indicating that affinity of hemoglobin for oxygen increases (mean decrease mitapivat 10  $\mu$ M

21.3±5.3%; tebapivat 10 µM 19.7±4.2%; tebapivat 2 µM 20.1±4.4%, all  $p < 0.0001$ ; **Figure 4A**, actual p50 values are depicted in **Supplemental Figure 5A**). We found no correlations between the decrease in p50 and decrease in 2,3-DPG, which could indicate that decreases in p50 are limited despite further decreasing 2,3-DPG levels (**Supplemental Figure 5B-D**).

Untreated whole blood of the HS patients showed the expected decreased  $EI_{max}$  in both the osmotic gradient ektacytometry and deformability assay, as well as a decreased  $\Delta EI$  in the CMST (data not shown). *Ex vivo* treatment with PK activators resulted in a significant decrease in  $EI_{max}$  (mitapivat 10 µM  $-0.9 \pm 0.7\%$ ,  $p < 0.001$ ; tebapivat 10 µM  $-1.2 \pm 0.8\%$ ,  $p = 0.0001$ ; tebapivat 2 µM  $-1.2 \pm 0.7\%$ ,  $p < 0.0001$ ; **Figure 4B**). In addition, we observed an increase in  $O_{min}$  (**Supplemental Figure 6A**). Importantly,  $O_{hyper}$  values significantly increased (mitapivat 10 µM  $2.1 \pm 0.8\%$ ; tebapivat 10 µM  $2.2 \pm 1.0\%$ ; tebapivat 2 µM  $2.4 \pm 0.7\%$ , all  $p < 0.0001$ ; **Figure 4C**) as well as  $O_{max}$  and AUC values (**Supplemental Figure 6B,C**). Together, these results indicate that PK activation improves RBC hydration. An illustrative osmotic gradient ektacytometry curve is depicted in **Supplemental Figure 6D**. No changes in deformability assay and CMST were observed (**Supplemental Figure 7A,B**).

In line with improvements in  $O_{hyper}$  and  $O_{max}$ , mean corpuscular volume (MCV) increased significantly (**Figure 4D**). In addition, we noted a decrease in MCHC and an increase in hypochromic cells (**Figure 4E,F**). No decrease in dense cells was observed (**Figure 4G**). Altogether, these results further support the conclusion that HS RBCs improve their hydration in response to PK activation. However, the densest cells may no longer be capable of improving their hydration.

HS RBCs are prone to adhere to laminin, an extracellular matrix protein in the spleen which traps RBCs.<sup>45</sup> Using a microfluidic assay, we observed that the number of adhered cells differed greatly between various patients. However, PK activation did not affect the number of adhered RBCs (**Figure 4H**). Increased calcium levels in RBCs are considered pathological and are, amongst other things, associated with dehydration via the Gardos effect.<sup>46</sup> We found no differences in calcium levels upon *ex vivo* treatment (**Figure 4I**).

### **Pyruvate kinase thermostability differs between splenectomized and non-splenectomized patients and correlates with reticulocyte percentage**

Splenectomy may alter the composition of the RBC population. We therefore compared splenectomized and non-splenectomized patients. Two outcomes significantly differed between the groups: PK activity and thermostability (**Figure 5A,B**). In non-splenectomized patients, PK thermostability was decreased when compared to HC (non-splenectomized HS  $63.8 \pm 9.9\%$  vs. HC  $78.6 \pm 3.7\%$ ,  $p < 0.05$ ) whereas in splenectomized patients thermostability was comparable to HC. PK thermostability response to mitapivat was significant in the splenectomized group, in contrast to the non-splenectomized group (**Figure 5C,D**). Tebapivat improved PK thermostability in both groups. We next investigated if changes in reticulocyte count could play a role as reticulocytes typically decrease upon splenectomy. Although there was no significant difference in reticulocyte percentage (**Figure 5E**), we did observe a significant negative correlation between PK thermostability and percentage of reticulocytes (both splenectomized and non-splenectomized pooled together) ( $r = -0.67$ ,  $p < 0.01$ ; **Figure 5F**). This suggests a relation between PK thermostability and RBC age. We also investigated whether disease severity may be related to PK properties and response to PK activation. In non-splenectomized

patients, three patients had a mild phenotype, two moderate and six severe. We found that PK/HK ratio was lower in 4 of the 6 severe patients, whilst PK thermostability and ATP/2,3-DPG ratio showed less evident differences (**Supplemental Figure 8A-C**). However, RBCs derived from severe patients did not respond differently to PK activation (**Supplemental Figure 8D-F**). In conclusion, our findings suggest a relation between PK thermostability and RBC age. PK properties may be compromised more in severely affected HS patients, yet the response to PK activation is similar for patients from all classes of disease severity.

## DISCUSSION

In this study, we demonstrate that RBCs derived from patients with HS have decreased PK activity. We are the first to show that upon *ex vivo* treatment with PK activators mitapivat and tebapivat, PK activity increases and PK thermostability improves. Enhanced PK activity is accompanied by a rise in ATP and, importantly, functional improvement, illustrated by improved hydration parameters. We also noted an increase in hemoglobin-oxygen affinity upon *ex vivo* treatment (in line with decreasing 2,3-DPG levels). However, the p50 value remained in a physiological range (similar to that of fetal hemoglobin).<sup>47</sup> Moreover, a recent study on SCD patients who were treated with mitapivat found no signs of impaired oxygen delivery.<sup>9</sup> Interestingly, when comparing splenectomized and non-splenectomized patients, we found that PK thermostability was most affected in the non-splenectomized patients.

As PK plays a key role in RBC metabolism, by generating ATP<sup>48-51</sup>, a decrease in activity may have a negative impact on overall functioning of the RBC. In HS, this may worsen RBC deformability and enhance splenic clearance. We thus hypothesize that, despite normal ATP/2,3-DPG ratios at baseline, PK activation and the subsequent increase in ATP will be beneficial. Another characteristic of PK, namely PK thermostability, was found to only be slightly decreased in non-splenectomized HS patients. The role of PK thermostability in HS remains unknown: we also did not observe that more severely affected patients have the most decreased PK thermostability. Interestingly, PK/HK ratio appeared to be lower in a few severe non-splenectomized cases. Nonetheless, RBCs from patients from all classes of disease severity responded similarly to *ex vivo* PK activation, suggesting that PK activation therapy may be beneficial across classes of disease severity.

The pre-clinical study of Matte et al. demonstrated that mitapivat ameliorated hemolysis in protein 4.2 deficient mice, a model for a HS that represents the phenotype, yet corresponds to a genotype that was not included in our human study and is rare in Europe.<sup>1,17</sup> RBC ion homeostasis was found to be improved, which could be related to our observed changes in hydration. Also, treatment partly restored the metabolome towards that of wild-type mice RBCs. Our study is the first to focus on metabolic response of human HS RBCs upon *ex vivo* treatment with a PK activator. Next to enhanced glycolysis, we found an increase in IMP. Activity of the enzyme AMP deaminase, which converts AMP to IMP, is enhanced upon increases in ATP and decreases in 2,3-DPG.<sup>52,53</sup> Whether increased IMP levels are of relevance remains to be investigated, as RBCs lack the ability to reconvert IMP into AMP.<sup>54</sup> Moreover, the observed changes in fatty acid components are intriguing, due to their role in membrane health, which is significantly impaired in HS.<sup>55</sup>

Overall, we obtained similar results for mitapivat and tebapivat, without any concentration-dependent effects for tebapivat. We did find that tebapivat has increased capability of enhancing PK thermostability compared to mitapivat, possibly due to its higher affinity, slower off-rate and more stabilizing binding to PK.<sup>15,27</sup> Whether this is clinically relevant remains to be investigated, as the mitapivat-treated RBCs also show responses in various outcomes (e.g., ATP, hydration and hemoglobin-oxygen affinity).

In various anemias, including HS, RBCs are dehydrated.<sup>56</sup> This contributes to premature clearance of RBCs. It could be hypothesized that ATP-dependent processes linked to

cellular hydration, such as the Na-K-ATPase pump, improve upon PK activation. Another hypothesis is that increased ATP levels could enhance calcium extrusion, via the plasma membrane calcium (PMCA) pump.<sup>46</sup> Despite no observed changes in calcium, it would be of interest to measure the activity of PMCA itself. Interestingly, we did not observe any improvements in percentage dense cells, possibly due their incapability to rehydrate.<sup>57</sup> Simultaneously we observed changes in  $O_{\min}$  and  $EI_{\max}$ , which we hypothesize to be related to increased hydration in RBCs that already have decreased membrane surface area. Notably, AUC improved. This parameter can be regarded as a cumulative reflection of various RBC properties associated with deformability and is decreased in HS.<sup>58,59</sup> Therefore, these observations further support the potential beneficial effects of PK activation. The clinical study should ultimately demonstrate whether these changes benefit RBC survival.

Another ATP-dependent process which may be influenced by PK activation is phosphorylation of membrane proteins.<sup>60</sup> Band 3, which plays a major role in HS pathophysiology, has several phosphorylation sites.<sup>61-63</sup> Phosphorylation of band 3 destabilizes the ankyrin-band 3-protein 4.2 complex, thus negatively impacting membrane stability.<sup>64,65</sup> Moreover, phosphorylation of band 3 has been demonstrated to regulate RBC glycolysis.<sup>66</sup> Recently, Le et al. described reduced band 3 phosphorylation in RBCs of SCD patients treated with mitapivat.<sup>67</sup> Future studies focusing on changes in phosphorylation upon PK activation could improve our understanding of how this may influence RBC deformability.

Currently, a clinical trial is ongoing in which adult patients with RBC membranopathies, including HS, are treated with mitapivat (SATISFY trial, NCT05935202).<sup>23</sup> The first results demonstrated improvements in hemoglobin and hemolytic markers.<sup>68</sup> In addition to safety and efficacy endpoints, functional parameters will be analyzed, including hemoglobin-oxygen affinity, osmotic gradient ektacytometry, and PK activity and thermostability. These outcomes will also be measured in RBC populations separated according to density.<sup>69</sup> Investigating different RBC subpopulations could provide insight in how reticulocytes and senescent RBCs respond to mitapivat treatment, which could be relevant regarding the correlation between reticulocytes and PK thermostability.

A major limitation in our study is the limited number of patients and genetic heterogeneity in our cohort. Although we did not find any differences in genotypic subgroups (data not shown), this should be further investigated. Simultaneously, being able to prove that PK can be activated and thus increases ATP levels in all RBCs, regardless of genotype, splenectomy status or disease severity, is of value.

The data presented here demonstrate a relative decreased activity of the key glycolytic enzyme PK in HS RBCs. Upon *ex vivo* activation of PK, ATP levels increased and RBC hydration improved. The results from the currently ongoing clinical study are highly anticipated. To better understand how PK activation affects RBC metabolism and subsequent functionality in HS, studies focusing on phosphorylation, membrane lipid composition and ion homeostasis are of interest. To conclude, our study is the first study demonstrating beneficial effects upon *ex vivo* PK activation treatment in human HS RBCs and supports the rationale for further investigation of PK activation in HS.

**ACKNOWLEDGMENTS:**

We thank Agios Pharmaceuticals Inc. for their support for this research. We would like to thank Robin van Bruggen, Boukje Beuger (both Sanquin Research and Landsteiner Laboratory, Amsterdam, The Netherlands) and Wassim El Nemer (Etablissement Français du Sang PACA-Corse, Aix-Marseille University, Marseille, France) for their advice and help with the laminin-binding assay.

**AUTHORSHIP CONTRIBUTIONS:**

MR and RvW designed and supervised the project, as well as acquired the funding for the project. JdW coordinated the project. JdW, TR, JB, MT and BvO performed experiments and collected data. JdW, TD, MT, EvB, MB and MR recruited patients and acquired patient data. JdW and TR performed the data analysis. JdW, MR and RvW wrote the original draft. All authors reviewed and edited the manuscript.

**DISCLOSURE OF CONFLICTS OF INTEREST:**

JdW, JB, MT, AG, EvB, MR and RvW receive research funding from Agios Pharmaceuticals Inc. EvB, MR and RvW are consultants for Agios Pharmaceuticals Inc. MW-R is a current employee of Agios Pharmaceuticals Inc. AG receives research funding from Agios, Bristol Myers Squibb, Saniona, and Sanofi and has done consulting for Agios, Bristol Myers Squibb, Novo Nordisk, Pharmacosmos, and Vertex Pharmaceuticals. MR and RvW have received research funding from Axcella Health and RR Mechatronics. RvW has done consulting for Pfizer.

**DATA AVAILABILITY STATEMENT:**

Data and protocols are available upon request (e-mail [r.vanwijk@umcutrecht](mailto:r.vanwijk@umcutrecht)). Data will be shared as is compliant with the General Data Protection Regulation and European Union privacy laws.

**ETHICS APPROVAL AND PATIENT CONSENT STATEMENT:**

This research was approved by the ethical committee of the University Medical Center Utrecht (NedMec, protocol number 21/793 and protocol number 18/774), according to the principles described in the declaration of Helsinki. All patients provided verbal and written consent for participation in this study.

## REFERENCES:

1. Perrotta S, Gallagher PG, Mohandas N. Hereditary spherocytosis. *The Lancet*. 2008;372(9647):1411-1426. doi:10.1016/S0140-6736(08)61588-3
2. Huisjes R, Bogdanova A, van Solinge WW, Schiffelers RM, Kaestner L, van Wijk R. Squeezing for Life – Properties of Red Blood Cell Deformability. *Front Physiol*. 2018;9. <https://www.frontiersin.org/journals/physiology/articles/10.3389/fphys.2018.00656>
3. Bolton-Maggs PHB, Langer JC, Iolascon A, Tittensor P, King MJ. Guidelines for the diagnosis and management of hereditary spherocytosis – 2011 update. *Br J Haematol*. 2012;156(1):37-49. doi:<https://doi.org/10.1111/j.1365-2141.2011.08921.x>
4. Guizzetti L. Total versus partial splenectomy in pediatric hereditary spherocytosis: A systematic review and meta-analysis. *Pediatr Blood Cancer*. 2016;63(10):1713-1722. doi:10.1002/PBC.26106
5. Tang X, Xue J, Zhang J, Zhou J. The efficacy of partial versus total splenectomy in the treatment of hereditary spherocytosis in children: a systematic review and meta-analysis. *Pediatr Surg Int*. 2024;40(1):1-11. doi:10.1007/S00383-024-05879-7/FIGURES/3
6. Al-Samkari H, Galactéros F, Glenthøj A, et al. Mitapivat versus Placebo for Pyruvate Kinase Deficiency. *New England Journal of Medicine*. 2022;386(15):1432-1442. doi:10.1056/NEJMOA2116634/SUPPL\_FILE/NEJMOA2116634\_DATA-SHARING.PDF
7. van Dijk MJ, Rab MAE, van Oirschot BA, et al. Safety and efficacy of mitapivat, an oral pyruvate kinase activator, in sickle cell disease: A phase 2, open-label study. *Am J Hematol*. 2022;97(7):E226-E229. doi:<https://doi.org/10.1002/ajh.26554>
8. Xu JZ, Conrey A, Frey I, et al. A phase 1 dose escalation study of the pyruvate kinase activator mitapivat (AG-348) in sickle cell disease. *Blood*. 2022;140(19):2053-2062. doi:10.1182/blood.2022015403
9. Idowu M, Otieno L, Dumitriu B, et al. Safety and efficacy of mitapivat in sickle cell disease (RISE UP): results from the phase 2 portion of a global, double-blind, randomised, placebo-controlled trial. *Lancet Haematol*. Published online December 4, 2024. doi:10.1016/S2352-3026(24)00319-3
10. Kuo KHM, Layton DM, Lal A, et al. Safety and efficacy of mitapivat, an oral pyruvate kinase activator, in adults with non-transfusion dependent  $\alpha$ -thalassaemia or  $\beta$ -thalassaemia: an open-label, multicentre, phase 2 study. *The Lancet*. 2022;400(10351):493-501. doi:[https://doi.org/10.1016/S0140-6736\(22\)01337-X](https://doi.org/10.1016/S0140-6736(22)01337-X)
11. Cappellini MD, Sheth S, Taher AT, et al. ENERGIZE-T: A Global, Phase 3, Double-Blind, Randomized, Placebo-Controlled Study of Mitapivat in Adults with Transfusion-Dependent Alpha- or Beta-Thalassemia. *Blood*. 2024;144(Supplement 1):409-409. doi:10.1182/BLOOD-2024-200867
12. Al-Samkari H, Fenaux P, Sekeres MA, et al. A Phase 2a/2b Multicenter Study of AG-946 in Patients with Anemia Due to Lower-Risk Myelodysplastic Syndromes. *Blood*. 2022;140(Supplement 1):4076-4078. doi:10.1182/BLOOD-2022-168907
13. Fattizzo B, Vercellati C, Marcello A, et al. Glycolytic activity and in vitro effect of the pyruvate kinase activator AG-946 in red blood cells from low-risk

- myelodysplastic syndromes patients: A proof-of-concept study. *Am J Hematol.* 2024;99(6):1201-1204. doi:10.1002/AJH.27300
14. van Dijk MJ, de Wilde JRA, Bartels M, et al. Activation of pyruvate kinase as therapeutic option for rare hemolytic anemias: Shedding new light on an old enzyme. *Blood Rev.* 2023;61:101103. doi:https://doi.org/10.1016/j.blre.2023.101103
  15. Kung C, Hixon J, Kosinski PA, et al. AG-348 enhances pyruvate kinase activity in red blood cells from patients with pyruvate kinase deficiency. *Blood.* 2017;130(11):1347-1356. doi:10.1182/blood-2016-11-753525
  16. Rab MAE, Bos J, van Oirschot BA, et al. Decreased activity and stability of pyruvate kinase in sickle cell disease: a novel target for mitapivat therapy. *Blood.* 2021;137(21):2997-3001. doi:10.1182/blood.2020008635
  17. Matte A, Wilson AB, Gevi F, et al. Mitapivat reprograms the RBC metabolome and improves anemia in a mouse model of hereditary spherocytosis. *JCI Insight.* 2023;8(20). doi:10.1172/jci.insight.172656
  18. van Dooijeweert B, Broeks MH, Verhoeven-Duif NM, et al. Metabolic Fingerprint in Hereditary Spherocytosis Correlates With Red Blood Cell Characteristics and Clinical Severity. *Hemasphere.* 2021;5(7). [https://journals.lww.com/hemasphere/fulltext/2021/07000/metabolic\\_fingerprint\\_in\\_hereditary\\_spherocytosis.2.aspx](https://journals.lww.com/hemasphere/fulltext/2021/07000/metabolic_fingerprint_in_hereditary_spherocytosis.2.aspx)
  19. Andres O, Loewecke F, Morbach H, et al. Hereditary spherocytosis is associated with decreased pyruvate kinase activity due to impaired structural integrity of the red blood cell membrane. *Br J Haematol.* 2019;187(3):386-395. doi:https://doi.org/10.1111/bjh.16084
  20. Lewis IA, Campanella ME, Markley JL, Low PS. Role of band 3 in regulating metabolic flux of red blood cells. *Proceedings of the National Academy of Sciences.* 2009;106(44):18515-18520. doi:10.1073/pnas.0905999106
  21. Puchulu-Campanella E, Chu H, Anstee DJ, Galan JA, Tao WA, Low PS. Identification of the Components of a Glycolytic Enzyme Metabolon on the Human Red Blood Cell Membrane \* . *Journal of Biological Chemistry.* 2013;288(2):848-858. doi:10.1074/jbc.M112.428573
  22. Glenthøj A, van Beers EJ, van Wijk R, et al. Designing a single-arm phase 2 clinical trial of mitapivat for adult patients with erythrocyte membranopathies (SATISFY): a framework for interventional trials in rare anaemias – pilot study protocol. *BMJ Open.* 2024;14(7):e083691. doi:10.1136/BMJOPEN-2023-083691
  23. Glenthøj A, Van Beers EJ, van Wijk R, et al. Safety and Efficacy of Mitapivat in Adult Patients with Erythrocyte Membranopathies (SATISFY). *Blood.* 2023;142(Supplement 1):1085. doi:10.1182/blood-2023-173147
  24. Eber SW, Armbrust R, Schröter W. Variable clinical severity of hereditary spherocytosis: relation to erythrocytic spectrin concentration, osmotic fragility, and autohemolysis. *J Pediatr.* 1990;117(3):409-416. doi:10.1016/S0022-3476(05)81081-9
  25. Beutler E. *Red Cell Metabolism. A Manual of Biochemical Methods.* . Third.; 1984.
  26. Rab MAE, van Oirschot BA, Kosinski PA, et al. AG-348 (Mitapivat), an allosteric activator of red blood cell pyruvate kinase, increases enzymatic activity, protein stability, and ATP levels over a broad range of PKLR genotypes. *Haematologica.* 2021;106(1):238-249. doi:10.3324/haematol.2019.238865

27. Liu T, Padyana AK, Judd ET, et al. Structure-Based Design of AG-946, a Pyruvate Kinase Activator. *ChemMedChem*. 2024;19(5):e202300559. doi:<https://doi.org/10.1002/cmdc.202300559>
28. Blume KG, Arnold H, Lohr GW, Beutler E. Additional diagnostic procedures for the detection of abnormal red cell pyruvate kinase. *Clinica Chimica Acta*. 1973;43(3):443-446. doi:[https://doi.org/10.1016/0009-8981\(73\)90487-7](https://doi.org/10.1016/0009-8981(73)90487-7)
29. van Wijk R, van Wesel ACW, Thomas AAM, Rijksen G, van Solinge WW. Ex vivo analysis of aberrant splicing induced by two donor site mutations in PKLR of a patient with severe pyruvate kinase deficiency. *Br J Haematol*. 2004;125(2):253-263. doi:<https://doi.org/10.1111/j.1365-2141.2004.04895.x>
30. Rijksen G, Schipper-Kester GPM, Staal GEJ, Veerman AJP. Diagnosis of pyruvate kinase deficiency in a transfusion-dependent patient with severe hemolytic anemia. *Am J Hematol*. 1990;35(3):187-193. doi:<https://doi.org/10.1002/ajh.2830350309>
31. Kim H, Kosinski P, Kung C, et al. A fit-for-purpose LC–MS/MS method for the simultaneous quantitation of ATP and 2,3-DPG in human K2EDTA whole blood. *Journal of Chromatography B*. 2017;1061-1062:89-96. doi:10.1016/J.JCHROMB.2017.07.010
32. de Sain-van der Velden MGM, van der Ham M, Gerrits J, et al. Quantification of metabolites in dried blood spots by direct infusion high resolution mass spectrometry. *Anal Chim Acta*. 2017;979:45-50. doi:10.1016/J.ACA.2017.04.038
33. Haijes HA, Willemsen M, van der Ham M, et al. Direct infusion based metabolomics identifies metabolic disease in patients' dried blood spots and plasma. *Metabolites*. 2019;9(1). doi:10.3390/METABO9010012
34. van Dijk MJ, Ruiter TJJ, van der Veen S, et al. Metabolic blood profile and response to treatment with the pyruvate kinase activator mitapivat in patients with sickle cell disease. *Hemasphere*. 2024;8(6):e109. doi:10.1002/HEM3.109
35. R Guarnone, E Centenara, G Barosi. Performance characteristics of Hemox-Analyzer for assessment of the hemoglobin dissociation curve. *Haematologica*. 1995;80(5):426-430. doi:10.3324/%x
36. Da Costa L, Suner L, Galimand J, et al. Diagnostic tool for red blood cell membrane disorders: Assessment of a new generation ektacytometer. *Blood Cells Mol Dis*. 2016;56(1):9-22. doi:10.1016/J.BCMD.2015.09.001
37. Berrevoets MC, Bos J, Huisjes R, et al. Ektacytometry Analysis of Post-splenectomy Red Blood Cell Properties Identifies Cell Membrane Stability Test as a Novel Biomarker of Membrane Health in Hereditary Spherocytosis. *Front Physiol*. 2021;12:641384. doi:10.3389/FPHYS.2021.641384/BIBTEX
38. Klei TRL, De Back DZ, Asif PJ, et al. Glycophorin-C sialylation regulates Lu/BCAM adhesive capacity during erythrocyte aging. *Blood Adv*. 2018;2(1):14. doi:10.1182/BLOODADVANCES.2017013094
39. Lizarralde-Iragorri MA, Lefevre SD, Cochet S, et al. Oxidative stress activates red cell adhesion to laminin in sickle cell disease. *Haematologica*. 2020;106(9):2478. doi:10.3324/HAEMATOL.2020.261586
40. Bianchi P, Fermo E, Glader B, et al. Addressing the diagnostic gaps in pyruvate kinase deficiency: Consensus recommendations on the diagnosis of pyruvate kinase deficiency. *Am J Hematol*. 2019;94(1):149-161. doi:<https://doi.org/10.1002/ajh.25325>

41. Al-Samkari H, Addonizio K, Glader B, et al. The pyruvate kinase (PK) to hexokinase enzyme activity ratio and erythrocyte PK protein level in the diagnosis and phenotype of PK deficiency. *Br J Haematol.* 2021;192(6):1092-1096. doi:<https://doi.org/10.1111/bjh.16724>
42. Bosman GJCGM, Lasonder E, Wisniewski JR. The Proteome of the Red Blood Cell: An Auspicious Source of New Insights into Membrane-Centered Regulation of Homeostasis. *Proteomes 2016, Vol 4, Page 35.* 2016;4(4):35. doi:10.3390/PROTEOMES4040035
43. Delivoria-Papadopoulos M, Oski FA, Gottlieb AJ. Oxygen-Hemoglobin Dissociation Curves: Effect of Inherited Enzyme Defects of the Red Cell. *Science (1979).* 1969;165(3893):601-602. doi:10.1126/SCIENCE.165.3893.601
44. Charache S, Grisolia S, Fiedler AJ, Hellegers AE. Effect of 2,3-diphosphoglycerate on oxygen affinity of blood in sickle cell anemia. *J Clin Invest.* 1970;49(4):806-812. doi:10.1172/JCI106294
45. Gauthier E, El Nemer W, Wautier MP, et al. Role of the interaction between Lu/BCAM and the spectrin-based membrane skeleton in the increased adhesion of hereditary spherocytosis red cells to laminin. *Br J Haematol.* 2010;148(3):456-465. doi:10.1111/J.1365-2141.2009.07973.X
46. Bogdanova A, Makhro A, Wang J, Lipp P, Kaestner L. Calcium in Red Blood Cells—A Perilous Balance. *International Journal of Molecular Sciences 2013, Vol 14, Pages 9848-9872.* 2013;14(5):9848-9872. doi:10.3390/IJMS14059848
47. Kaufman DP, Khattar J, Lappin SL. Physiology, Fetal Hemoglobin. *StatPearls.* Published online March 20, 2023. Accessed September 3, 2024. <https://www.ncbi.nlm.nih.gov/books/NBK500011/>
48. Van Wijk R, Van Solinge WW. The energy-less red blood cell is lost: erythrocyte enzyme abnormalities of glycolysis. *Blood.* 2005;106(13):4034-4042. doi:10.1182/BLOOD-2005-04-1622
49. Martinov M V., Plotnikov AG, Vitvitsky VM, Ataulakhanov FI. Deficiencies of glycolytic enzymes as a possible cause of hemolytic anemia. *Biochimica et Biophysica Acta (BBA) - General Subjects.* 2000;1474(1):75-87. doi:10.1016/S0304-4165(99)00218-4
50. Weed RI, LACEILLE PL, Gael Craib M, Ann Gregory M, Fred Karch M, Franges Pickens M. Metabolic dependence of red cell deformability. *J Clin Invest.* 1969;48(5):795-809. doi:10.1172/JCI106038
51. Park YK, Best CA, Auth T, et al. Metabolic remodeling of the human red blood cell membrane. *Proc Natl Acad Sci U S A.* 2010;107(4):1289-1294. doi:10.1073/PNAS.0910785107/SUPPL\_FILE/SM4.MOV
52. Yun S, Suelter CH. Human erythrocyte 5'-AMP aminohydrolase. Purification and characterization. *Journal of Biological Chemistry.* 1978;253(2):404-408. doi:10.1016/S0021-9258(17)38223-6
53. Lian CY, Harkness DR. The kinetic properties of adenylate deaminase from human erythrocytes. *BBA - Enzymology.* 1974;341(1):27-40. doi:10.1016/0005-2744(74)90062-X
54. Lowy B, Dorfman BZ. Adenylosuccinase activity in human and rabbit erythrocyte lysates. *Journal of Biological Chemistry.* 1970;245(12):3043-3046. doi:10.1016/s0021-9258(18)63020-0

55. Mohandas N, Gallagher PG. Red cell membrane: past, present, and future. *Blood*. 2008;112(10):3939-3948. doi:10.1182/BLOOD-2008-07-161166
56. Gallagher PG. Disorders of erythrocyte hydration. *Blood*. 2017;130(25):2699-2708. doi:10.1182/BLOOD-2017-04-590810
57. Lew VL, Tiffert T. The terminal density reversal phenomenon of aging human red blood cells. *Front Physiol*. 2013;4 JUL:57944. doi:10.3389/FPHYS.2013.00171/BIBTEX
58. Zaninoni A, Fermo E, Vercellati C, et al. Use of laser assisted optical rotational cell analyzer (LoRRca MaxSis) in the diagnosis of RBC membrane disorders, enzyme defects, and congenital dyserythropoietic anemias: A monocentric study on 202 patients. *Front Physiol*. 2018;9(APR):354553. doi:10.3389/FPHYS.2018.00451/BIBTEX
59. Llaudet-Planas E, Vives-Corrans JL, Rizzuto V, et al. Osmotic gradient ektacytometry: A valuable screening test for hereditary spherocytosis and other red blood cell membrane disorders. *Int J Lab Hematol*. 2018;40(1):94-102. doi:10.1111/IJLH.12746
60. Cilek N, Ugurel E, Goksel E, Yalcin O. Signaling mechanisms in red blood cells: A view through the protein phosphorylation and deformability. *J Cell Physiol*. 2024;239(3):e30958. doi:https://doi.org/10.1002/jcp.30958
61. Pantaleo A, Ferru E, Pau MC, et al. Band 3 Erythrocyte Membrane Protein Acts as Redox Stress Sensor Leading to Its Phosphorylation by p72 Syk. *Oxid Med Cell Longev*. 2016;2016(1):6051093. doi:10.1155/2016/6051093
62. Moura PL, Iragorri MAL, Français O, et al. Reticulocyte and red blood cell deformation triggers specific phosphorylation events. *Blood Adv*. 2019;3(17):2653-2663. doi:10.1182/BLOODADVANCES.2019000545
63. De Franceschi L, Tomelleri C, Matte A, et al. Erythrocyte membrane changes of chorea-acanthocytosis are the result of altered Lyn kinase activity. *Blood*. 2011;118(20):5652-5663. doi:10.1182/BLOOD-2011-05-355339
64. Ferru E, Giger K, Pantaleo A, et al. Regulation of membrane-cytoskeletal interactions by tyrosine phosphorylation of erythrocyte band 3. *Blood*. 2011;117(22):5998-6006. doi:10.1182/BLOOD-2010-11-317024
65. Noomuna P, Risinger M, Zhou S, et al. Inhibition of Band 3 tyrosine phosphorylation: a new mechanism for treatment of sickle cell disease. *Br J Haematol*. 2020;190(4):599. doi:10.1111/BJH.16671
66. Harrison ML, Rathinavelu P, Arese P, Geahlen RL, Low PS. Role of band 3 tyrosine phosphorylation in the regulation of erythrocyte glycolysis. *Journal of Biological Chemistry*. 1991;266(7):4106-4111. doi:10.1016/s0021-9258(20)64292-2
67. Le K, Wang X, Chu J, et al. Activating pyruvate kinase improves red blood cell integrity by reducing band 3 tyrosine phosphorylation. *Blood Adv*. Published online September 12, 2024. doi:10.1182/BLOODADVANCES.2024013504
68. Doeven T, Van Beers EJ, van Wijk R, et al. Satisfy: A Eurobloodnet Multicenter, Single-Arm Phase 2 Trial of Mitapivat in Adult Patients with Erythrocyte Membranopathies and Congenital Dyserythropoietic Anemia Type II - Results from the 8-Week Dose-Escalation Period. *Blood*. 2024;144(Supplement 1):3831-3831. doi:10.1182/BLOOD-2024-198359
69. Bosch F, Werre J, Roerdinkholder-Stoelwinder B, Huls T, Willekens F, Halie M. Characteristics of Red Blood Cell Populations Fractionated With a Combination of

Counterflow Centrifugation and Percoll Separation. *Blood*. 1992;79(1):254-260.  
doi:10.1182/BLOOD.V79.1.254.254

## TABLE LEGEND

### **Table 1 - Characteristics of the included hereditary spherocytosis patients.**

In total, blood samples from 18 patients were collected. Genotype, treatment and general hematological indices per patients are described (with reference ranges for the latter). The type of mutation (missense (M), nonsense (N) or splice site (S)) is noted with the mutation.

C cobalamin; F female; FA folic acid; Hb hemoglobin; M male; RBC red blood cells; Ret reticulocytes. \*Disease severity was based on hemoglobin values and reticulocyte percentages.

**TABLES:**

**Table 1 - Characteristics of the included hereditary spherocytosis patients.**

Patient	Age	Sex	Affected gene	Mutation	Family	Splenectomy	Treatment	Hb (g/dL)	RBC (x10 <sup>12</sup> /L)	Ret. (%)	Severity*
HS01	54	F	<i>ANK1</i>	c.344T>C, p.Leu115Pro) (M)	1	Yes	FA	13.58	4.50	2.96	NA
HS02	43	F	<i>SPTB</i>	c.4789C>T, p.Gln1660*) (N)	2	Yes	None	13.12	5.32	3.64	NA
HS03	38	F	<i>SLC4A1</i>	c.106+1G>A, p.(?) (S)	3	No	FA	9.75	2.92	5.19	Moderate
HS04	68	F	<i>SPTB</i>	c.4789C>T, p.(Gln1660*) (N)	2	Yes	None	14.49	4.69	2.12	NA
HS05	33	F	<i>ANK1</i>	c.856C>T p.(Arg286*) (N)	4	No	FA	12.55	4.36	10.3	Mild
HS06	35	F	<i>ANK1</i>	c.3G>T p.(Met1*) (N)	5	No	FA	8.17	3.11	13.1	Severe
HS07	67	M	<i>ANK1</i>	c.856C>T p.(Arg286*) (N)	4	Yes	None	17.56	5.63	7.28	NA
HS08	42	F	<i>SPTB</i>	c.5128G>T p.(Glu1710*) (N)	6	Yes	None	15.57	5.27	8.15	NA
HS09	37	M	<i>SLC4A1</i>	c.106+1G>A, p.(?) (S)	3	No	FA	15.53	5.01	4.32	Mild
HS10	66	F	<i>SLC4A1</i>	c.106+1G>A, p.(?) (S)	3	No	FA	12.67	4.02	8.57	Moderate

HS11	65	M	<i>SPTB</i>	c.5128G>T p.(Glu1710*) (N)	6	Yes	FA, C	16.08	5.09	14.7	NA
HS12	36	F	<i>SPTB</i>	c.5128G>T p.(Glu1710*) (N)	6	No	FA	11.31	3.68	27.3	Severe
HS13	46	M	<i>SPTB</i>	c.5128G>T p.(Glu1710*) (N)	6	Yes	None	15.37	4.88	11.8	NA
HS14	39	F	<i>SLC4A1</i>	c.1271G>A p.(Gly424Asp) (M)	7	No	FA	11.47	3.07	18.4	Severe
HS15	45	M	<i>SPTB</i>	c.647G>A p.(Arg216Gln) (M)	8	No	None	12.46	4.14	14.1	Severe
HS16	30	M	<i>ANK1</i>	c.2632G>T p.(Glu878*) (N)	9	No	None	10.52	3.79	15.6	Severe
HS17	24	F	<i>SPTB</i>	c.155G>A p.(Arg52Gln) (M)	10	No	FA	10.22	3.43	14.7	Severe
HS18	40	F	<i>SPTA1</i>	c.2806-13T>G p.(?) (S)	11	No	FA, C	11.54	3.70	5.49	Mild
Reference ranges								M 13.9- 17.2 F 11.9-15.5	M 4-5.9 F 3.8-5.2	1-2.5	

## FIGURE LEGENDS.

### Figure 1 - Pyruvate kinase characteristics in untreated hereditary spherocytosis red blood cells.

(A,B) Pyruvate kinase (PK) activity was determined in hereditary spherocytosis (HS, N=18) red blood cells (RBCs) and was compared to healthy controls (HC, N=12). (B) (C,D) To assess PK function, the PK/hexokinase (HK) ratio is calculated, to correct for RBC age. (E,F) Another aspect of PK, PK thermostability, was assessed in both HS and HC (N=6). (G,H) Also the adenosine triphosphate (ATP)/2,3-diphosphoglycerate (2,3-DPG) ratio was compared between patients and HC (N=6).

<sup>†</sup>Patients are splenectomized.

ATP adenosine triphosphate; DPG diphosphoglycerate; HC healthy controls; HK hexokinase; HS hereditary spherocytosis; PK pyruvate kinase. Error bars represent standard deviation. \* $p < 0.05$ , \*\*\*\* $p < 0.0001$ , ns not significant.

### Figure 2 - Activation of pyruvate kinase in hereditary spherocytosis red blood cells enhances energy metabolism.

(A,B) Red blood cells (RBCs) were treated *ex vivo* with the pyruvate kinase (PK) activators mitapivat 10  $\mu\text{M}$  and tebapivat 10 and 2  $\mu\text{M}$  overnight, after which PK and hexokinase (HK) activity were measured (N=18). (C) PK thermostability was assessed, upon treatment of RBC lysates for 2 hours (N=17). Lower concentrations of PK activators were used (mitapivat 2  $\mu\text{M}$ , tebapivat 2  $\mu\text{M}$  and 500 nM). (D) The PK thermostability at different timepoints is displayed. Again, lower concentrations of the compounds were used. (E-G) Upon PK activation, adenosine triphosphate (ATP) and 2,3-diphosphoglycerate (2,3-DPG) levels were measured, and the changes in these metabolites as well as in the ATP/2,3-DPG ratio was calculated (N=13).

ATP adenosine triphosphate; DMSO dimethylsulfoxide; DPG diphosphoglycerate; HK hexokinase; PEP phosphoenolpyruvate; PK pyruvate kinase. Error bars represent standard deviation. \*\* $p < 0.01$ , \*\*\*\* $p < 0.0001$ , ns not significant.

### Figure 3 – Metabolic changes in hereditary spherocytosis red blood cells upon *ex vivo* treatment with tebapivat 2 $\mu\text{M}$ compared to vehicle.

(A) Principal component analysis of hereditary spherocytosis (HS) red blood cells (RBCs) treated with either DMSO (vehicle, red) or tebapivat 2  $\mu\text{M}$  (light pink) displayed with 95% confidence regions (N=15). Sample names are displayed, and each number corresponds to an individual sample. (B) Volcano plot showing metabolites that significantly increase (red) or decrease (blue) upon *ex vivo* treatment with tebapivat. Vertical dotted lines represent  $p$ -value cut-off of 0.05 (unadjusted), indicating statistical significance, and horizontal dotted lines represent fold-change cut-off of 2.0, indicating biological significance. (C) Heatmap of the 50 most significantly different metabolites between DMSO (vehicle) or tebapivat 2  $\mu\text{M}$  treated HS RBCs as identified by paired t-tests (unadjusted  $p < 0.05$ ). A comprehensive overview of  $p$ -values and isomers is displayed in Supplemental File 2.

DG diglyceride; DMSO dimethylsulfoxide; DPG diphosphoglycerate; FC fold change; HS hereditary spherocytosis; IMP inosine monophosphate; LysoPC Lysophosphatidyl ethanolamine; LysoPE lysophosphatidyl ethanolamine; MG monoglyceride; PC principal component; PEP phosphoenolpyruvate; PG phosphoglycerate; RBC red blood cell.

**Figure 4 – Enhanced glycolysis affects various red blood cell characteristics.**

(A) The change in hemoglobin-oxygen affinity was measured (change in p50) (N=16). (B,C) To test the functional response of red blood cells (RBCs) to the *ex vivo* treatment, osmotic gradient ektacytometry parameters were analyzed ( $EI_{max}$  and  $O_{hyper}$ ) (N=15). (D-G) To further explore the effect of pyruvate kinase (PK) activation on hydration, mean corpuscular volume (MCV), mean corpuscular hemoglobin concentration (MCHC), percentage of hypochromic cells and percentage of dense cells were measured (N=16 for MCV and MCHC, N=14 for percentage hypochromic and dense cells). (H) Changes in the number of RBCs adhered to laminin were analyzed (N=13). (I) The intracellular calcium concentration was determined and compared between the treatment groups (N=10).

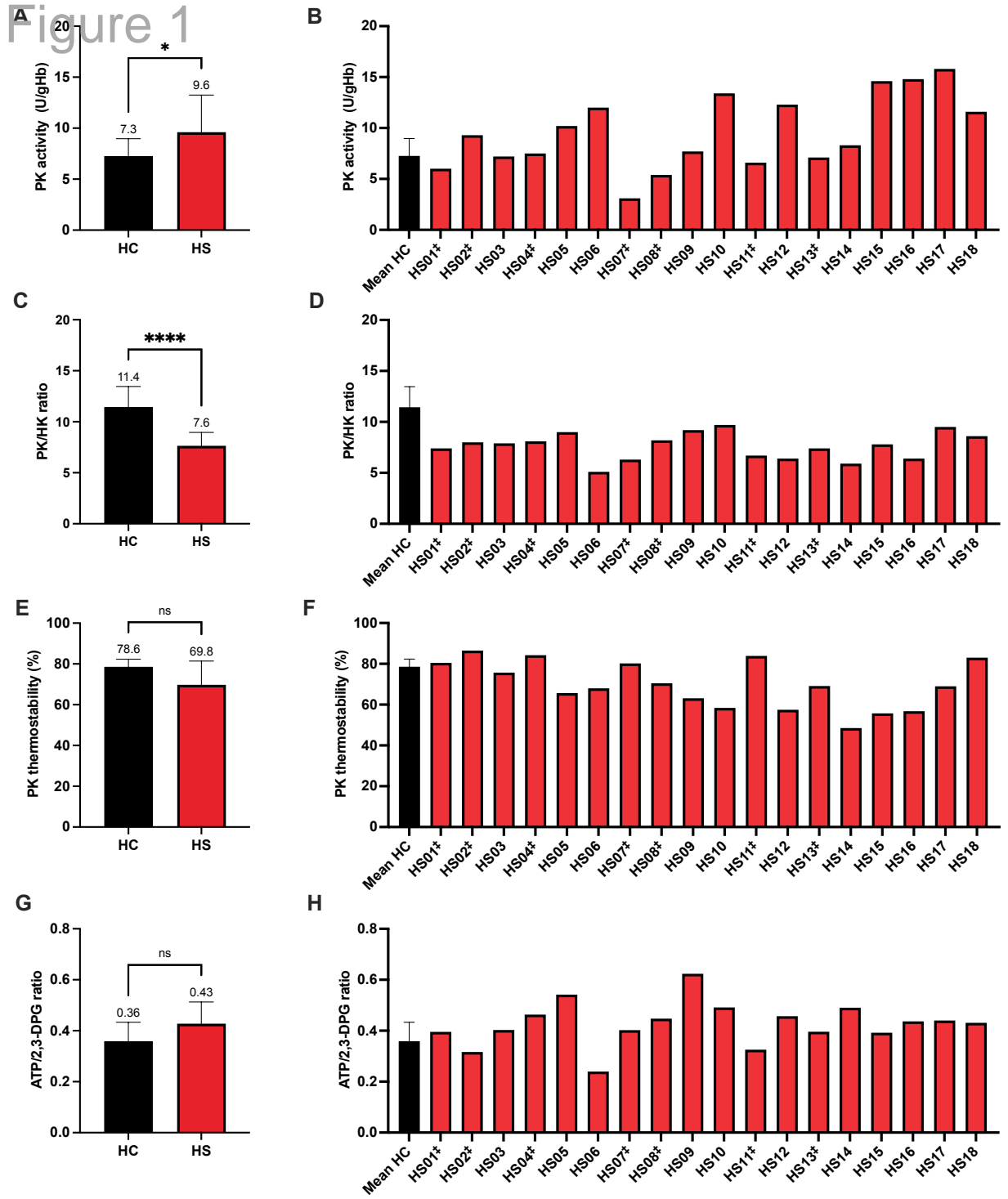
DMSO dimethylsulfoxide; EI elongation index; MCHC mean corpuscular hemoglobin concentration; MCV mean corpuscular volume; MFI mean fluorescence intensity; RBCs red blood cells. Error bars represent standard deviation. \* $p < 0.05$ , \*\* $p < 0.01$ , \*\*\* $p < 0.001$ , \*\*\*\* $p < 0.0001$ , ns not significant.

**Figure 5 – Differences between splenectomized and non-splenectomized patients in pyruvate kinase characteristics and responses to *ex vivo* activation.**

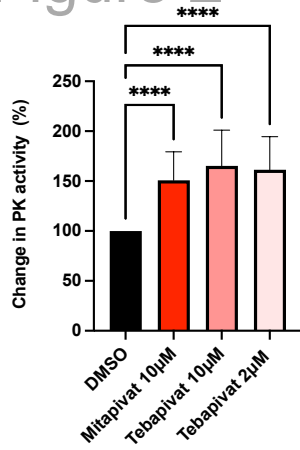
(A,B) The pyruvate kinase (PK) activity and thermostability (phosphoenolpyruvate (PEP) 5 mM) of untreated red blood cells in splenectomized hereditary spherocytosis (HS) patients (N=7) were compared to non-splenectomized patients (N=11) and healthy controls (HC, N=12 for activity and N=6 for thermostability). (C,D) Response of *ex vivo* treatment on PK thermostability (PEP 0.5 mM) evaluated in the splenectomized (N=7) and non-splenectomized group (N=11). (E) Differences in reticulocyte percentage between the total, splenectomized and non-splenectomized patients are shown. (F) The relation between reticulocyte percentage and PK thermostability shows a strong negative correlation. Squared symbols represent the splenectomized patients.

DMSO dimethylsulfoxide; HC healthy controls; HS hereditary spherocytosis; PK pyruvate kinase. Error bars represent standard deviation. \* $p < 0.05$ , \*\* $p < 0.01$ , \*\*\*\* $p < 0.0001$ , ns not significant.

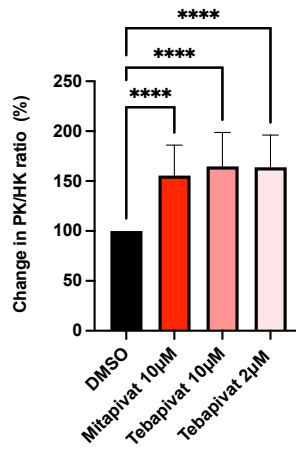
**Figure 1**



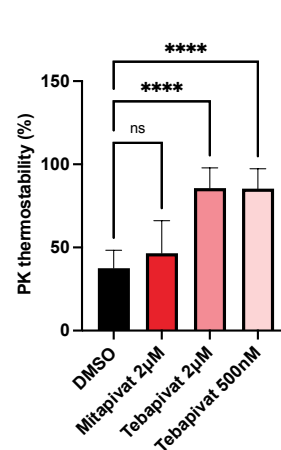
**A** Figure 2



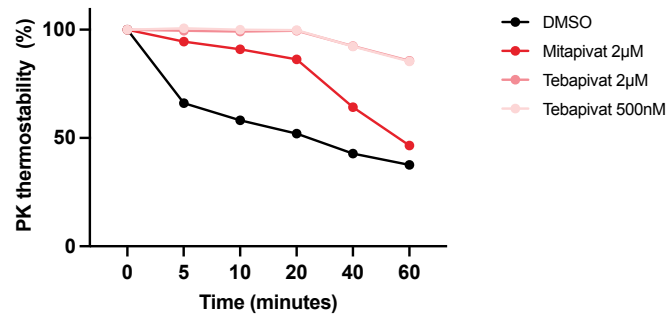
**B**



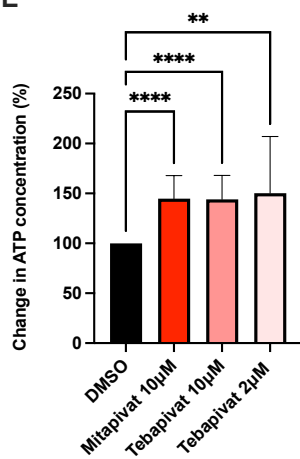
**C**



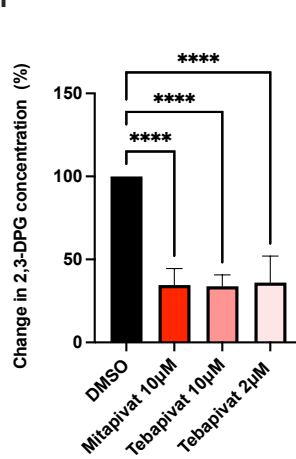
**D**



**E**



**F**



**G**

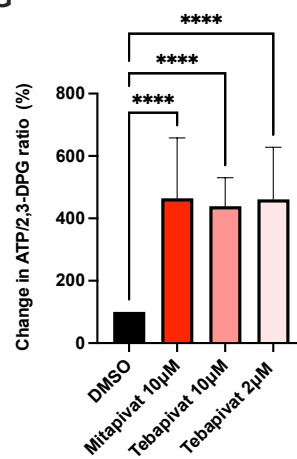




Figure 4

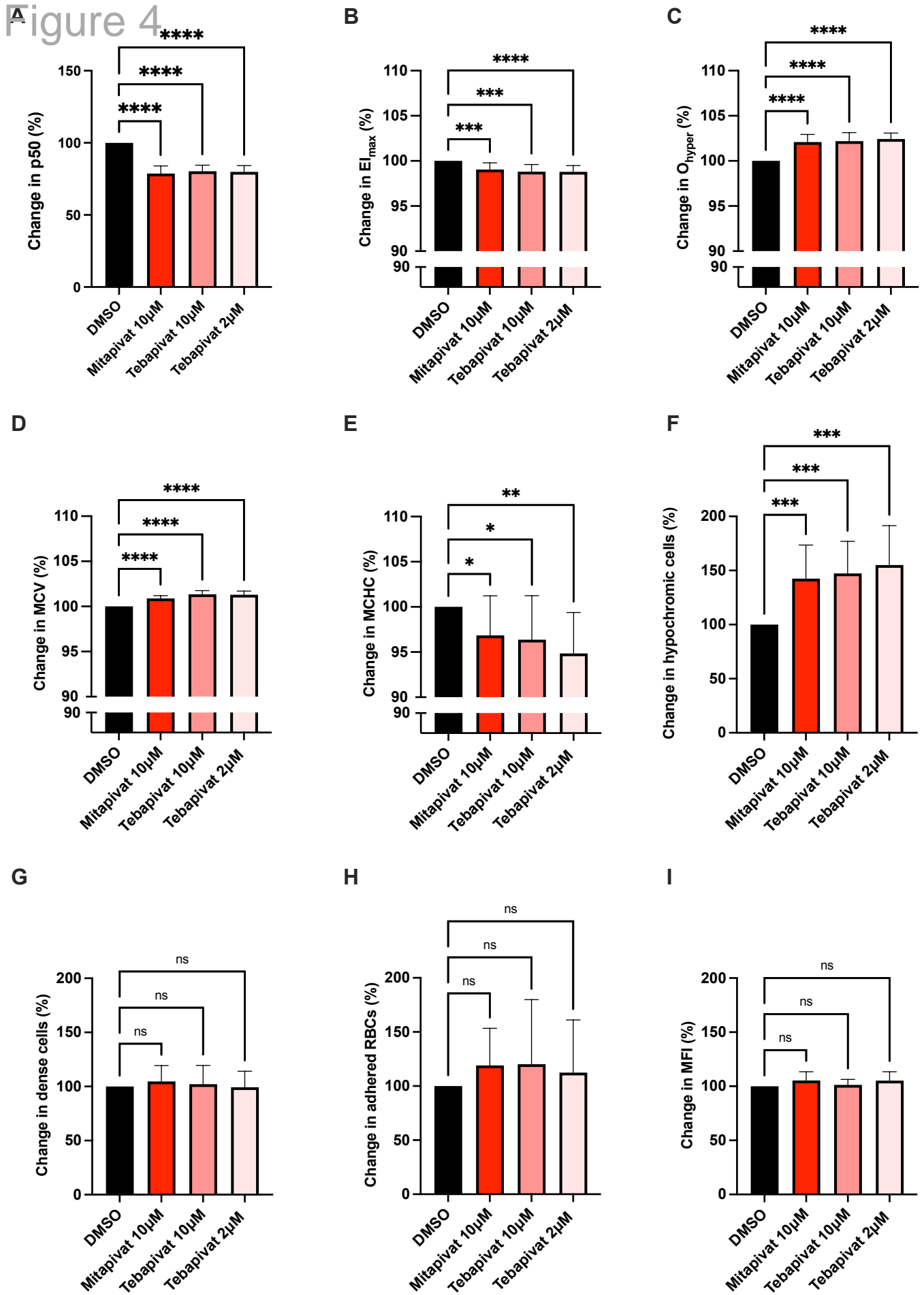
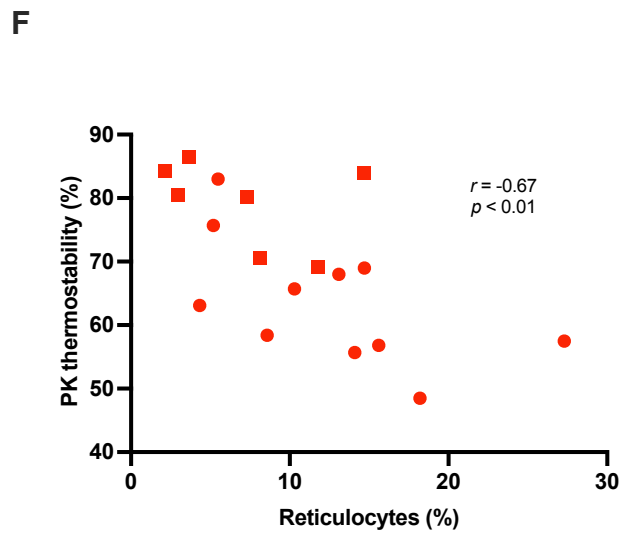
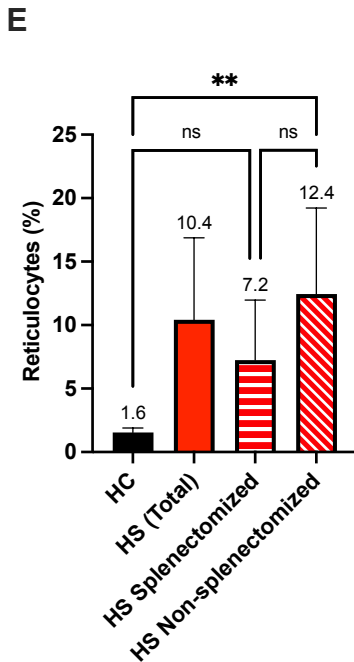
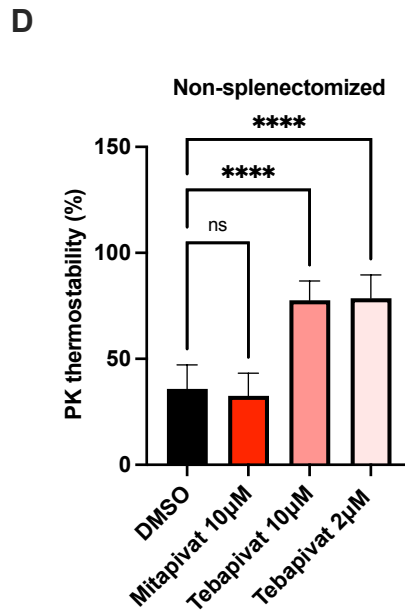
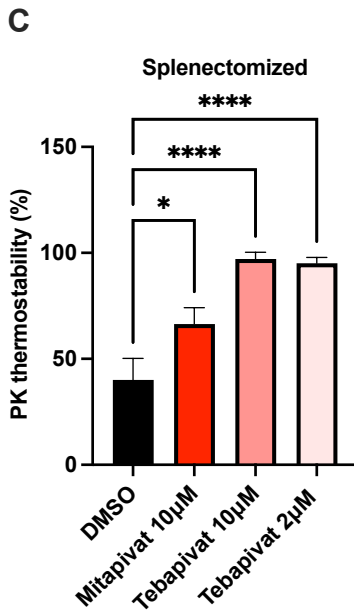
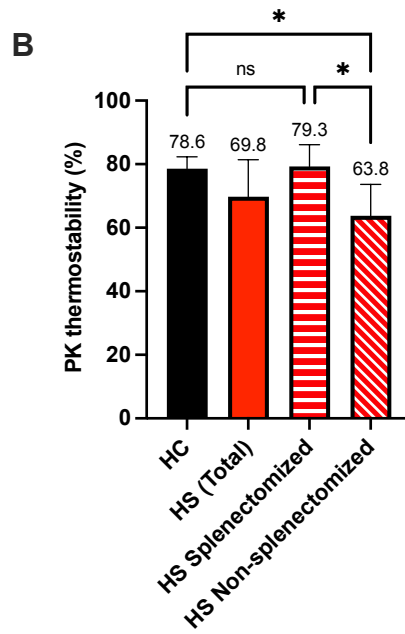
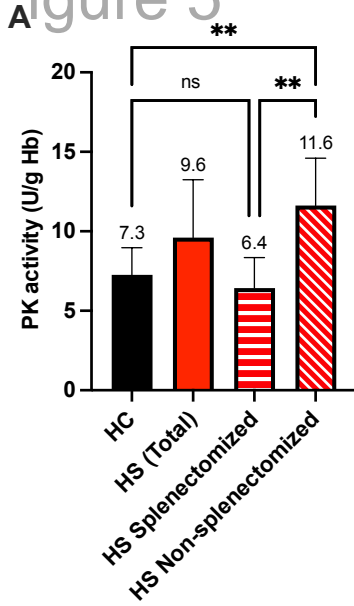


Figure 5



## **SUPPLEMENTAL FILES.**

### **SUPPLEMENTAL METHODS.**

#### **Red blood cell purification**

Whole blood was collected in 10 mL lithium-heparin tubes. Three 10 mL whole blood tubes were then centrifuged (500 G for 5 minutes), after which plasma was removed. To ensure that we preserve the denser and poorly deformable red blood cells (RBCs), the plasma-depleted blood was divided in two parts. The upper part (defined as buffy coat and the first two centimeters of RBCs below the buffy coat) was then transferred to a PD10 column (Cytiva) containing a cellulose mixture (1:1 alpha-cellulose and type 50 cellulose, Sigma-Aldrich) as well as a filter. This PD10 column was placed in a 50 mL Falcon tube. This upper part was then centrifuged (50 G for 5 minutes), additional saline (0.9%) was added, and the centrifugation step was repeated. The RBCs pass the cellulose mixture and filter and thus are located in the bottom of the Falcon tube. After removal of the PD10 column (containing the cellulose mixture with white blood cells (WBCs) and platelets), the RBCs are washed (twice, 350 G for 10 minutes) with saline 0.9% to remove the remaining platelets. These last two washing steps are also performed for the lower part of the centrifuged whole blood, which are the denser RBCs. After these washing steps, both RBC fractions are combined. Routine hematological parameters are measured to determine if the RBC purification was successful. When the number of WBCs exceeds the criteria ( $\geq 1.0 \times 10^9$  WBCs/L per  $4.0 \times 10^{12}$  RBCs/L), the whole process was repeated. When the number of platelets exceeds our limits ( $\geq 20 \times 10^9$  platelets/L per  $4.0 \times 10^{12}$  RBCs/L), only the washing step is repeated.

#### **Pyruvate kinase activity, thermostability and quantity**

For enzyme activity measurements, the method of Beutler was used. RBC lysates were prepared by lysing purified RBCs in beta-mercapto stabilizing solution to a hemoglobin concentration of  $\pm 1.0$  g/dL. For the pyruvate kinase (PK) activity measurement, lysates were then diluted (1:10) in a mixture containing 6 units lactate dehydrogenase (LDH, Roche), 0.2 mM nicotinamide adenine dinucleotide (NADH, Roche), 100 mM KCl, 10 mM  $MgCl_2$ , 1.5 mM adenosine diphosphate (ADP, Sigma-Aldrich) and 0.1 mM Tris-HCl/ 0.5 mM EDTA, final pH 8.0. The enzymatic reaction cascade is initiated by the adding of phosphoenolpyruvate (PEP, Merck) to the mixture, upon which the decrease of NADH can be kinetically measured using a spectrophotometer (Spectramax iD3, Molecular Devices) at 340 nm. Both PEP 5 mM final concentration ( $V_{max}$  condition) and PEP 0.5 mM final concentration (suboptimal conditions) are used. Hexokinase (HK) activity is also measured, as both PK and HK are age-dependent enzymes, implicating that activity of both enzymes decrease as RBCs age. The usage of the PK/HK ratio is thus used to evaluate PK activity in light of RBC age. For HK, RBC lysates are diluted (1:10) in a mixture containing 0.1 units glucose-6-phosphate dehydrogenase (G6PD, Roche), 0.2 mM nicotinamide adenine dinucleotide phosphate (NADP, Roche), 2 mM glucose, 10 mM  $Mg^{2+}$ , 10 mM adenosine triphosphate (ATP, Roche) and 0.1 mM Tris-HCl/ 0.5 mM EDTA, final pH 8.0. The activity of HK can be determined by kinetically measuring the increase in NADPH using a spectrophotometer at 340 nm. Measured activities are corrected for hemoglobin concentration and are expressed as units per gram hemoglobin (i.e., the specific enzyme activity).

The PK thermostability measurement is used to assess the stability of the enzyme. Here, RBC lysates (prepared as described above) were first incubated at 37 °C for 2 hours with either vehicle (DMSO 0.1%), mitapivat 2 μM, tebapivat 2 μM or tebapivat 500 nM final concentration. Next, these lysates were incubated at 53 °C and at different time intervals (0, 5, 10, 20, 40 and 60 minutes) lysate was collected. After chilling of the collected lysate (in ice water for 5 minutes) and centrifugation (600 G for 3 minutes), PK activity was measured in the supernatant (as described above, using both 5 and 0.5 mM PEP final concentration). The main outcome for this assay is the residual activity (expressed as PK thermostability in percentage) after 60 minutes incubation at 53 °C compared to time point 0 minutes. To compare PK thermostability between hereditary spherocytosis (HS) and healthy controls (HC), the PK thermostability ( $V_{max}$  condition) of the vehicle-treated lysate was compared between HS and HC RBC lysate. To assess the effect of the PK activators on PK thermostability, the PK thermostability at PEP 0.5 mM final concentration was used.

For the western blot analysis of PKR and PKM2, the antibodies used were rabbit anti-PKRL (gifted by the late dr. Kahn), mouse IgG anti-PKM2 (Podiceps) and mouse IgM anti-actin (Calbiochem) as loading control. Protein bands were visualized using respectively anti-rabbit IgG (Life), anti-mouse IgG (Life) and anti-mouse IgM (Life). Protein content was quantified using Odyssey M Infrared Imaging System (Li-Cor Biosciences).

### **Measurements of adenosine triphosphate and 2,3-diphosphoglycerate**

The standard calibration curve of 2,3-DPG and ATP ranged from 2.0 to 0.004 mg/mL. 20 μL sample (whole blood) or 20 μL of calibration standard were diluted in 200 μL water. To each sample and calibration standard, 20 μL of the internal standard solution was added, which contained 1 mg/mL  $^{13}\text{C}_{10}^{15}\text{N}_5$ -ATP (Merck) and 0.2 mg/mL  $^{13}\text{C}_3$ -2,3-DPG (Toronto Research Chemicals). Then 800 μL methanol was added and all samples were vortexed and centrifuged (17000 G for 10 minutes at 4 °C). 200 μL of the supernatant was transferred to a new Eppendorf tube and 800 μL acetonitrile was added. Samples were again vortexed and centrifuged (17000 G for 10 minutes at 4 °C). The supernatant was then analyzed using an Ultimate 3000 UHPLC system (Thermo Fisher Scientific) coupled to a Q Exactive™ HF hybrid quadrupole Orbitrap mass spectrometer (Thermo Fisher Scientific). Chromatic separation was performed using a BioBasic AX column (2.1 x 50 mm, 5 μm, Thermo Fisher Scientific). Solvent A was 5 mM ammonium acetate in acetonitrile/ultrapure H<sub>2</sub>O (20/80) containing 0.1% acetic acid, and solvent B was 10 mM ammonium acetate in acetonitrile/ultrapure H<sub>2</sub>O (20/80) containing 0.5% ammonium hydroxide. The column temperature was 40 °C with a flow rate of 0.6 mL/min and the following gradient: linear from 30 to 50% B from 0 to 1.5 min, linear from 50 to 100% B from 1.5 to 2.0 min, isocratic 100% B from 2.0 to 3.5 min, linear from 100 to 30% B from 3.5 to 3.6 min, isocratic 30% B (initial solvent conditions) from 3.6 to 5.5 min to equilibrate the column. Metabolites were detected using an electrospray ionization source operating in negative mode over a scan range of 200–600 mass to charge ratio (m/z). Scan parameters included a resolution of 120.000, AGC target value of  $3 \times 10^6$ , maximum injection time of 200 ms, capillary (kV) 4.0 in both positive and negative ion mode, capillary temperature of 350 °C, and a factor of 75 was used for the S-lens RF level. Data were acquired using Xcalibur software (version 3.0; Thermo Fisher Scientific). For the

integration of raw data peaks, TraceFinder 4.1 software (Thermo Fisher Scientific) was used.

### **Untargeted metabolomics**

Whole blood and *ex vivo* treated RBCs ( $3.6 \times 10^{12}$  RBCs/L) were spotted on a filter paper (Whatman Grade F-12), 50  $\mu$ L per spot. After drying at room temperature for 4 hours, the filter papers were stored at  $-80$  °C in a foil bag with a desiccant package. For untargeted metabolomic analysis, a 3 mm punch was collected from these dried blood spots (DBS), containing approximately 3.1  $\mu$ L of blood. 140  $\mu$ L of a working solution containing stable isotope-labeled compounds in methanol was added to the DBS (25  $\mu$ M  $^{15}\text{N}$ ;2- $^{13}\text{C}$ -glycine, 5  $\mu$ M  $^2\text{H}_4$ -alanine,  $^2\text{H}_4$ -valine,  $^2\text{H}_3$ -leucine,  $^2\text{H}_3$ -methionine,  $^{13}\text{C}_6$ -phenylalanine,  $^{13}\text{C}_6$ -tyrosine,  $^2\text{H}_3$ -aspartate,  $^2\text{H}_3$ -glutamate,  $^2\text{H}_2$ -ornithine,  $^2\text{H}_2$ -citrulline, and  $^2\text{H}_4$ ;  $^{13}\text{C}$ -arginine, 1.52  $\mu$ M  $^2\text{H}_9$ -carnitine, 0.38  $\mu$ M  $^2\text{H}_3$ -acetylcarnitine, 0.076  $\mu$ M  $^2\text{H}_3$ -propionylcarnitine,  $^2\text{H}_3$ -butyrylcarnitine,  $^2\text{H}_9$ -isovalerylcarnitine,  $^2\text{H}_3$ -octanoylcarnitine,  $^2\text{H}_9$ -myristoylcarnitine, and 0.152  $\mu$ M  $^2\text{H}_3$ -palmitoylcarnitine (Cambridge Isotope Laboratories), followed by a twenty minute ultra-sonication step for metabolite extraction. 60  $\mu$ L of 0.3% formic acid was added and then samples were filtered using a vacuum manifold and a 96-well filter plate (Pall Corporation) preconditioned with methanol. Filtered samples were collected in an Armadillo high-performance 96-well PCR plate (Thermo Fisher Scientific) and subjected to direct-infusion high-resolution mass spectrometry (DI-HRMS) using a TriVersa NanoMate system (Advion) connected to the interface of a Q Exactive high-resolution mass spectrometer (Thermo Scientific). Run time was 3 minutes during which the samples were measured in both negative and positive ion modus over a scan range of 70 to 600 mass to charge ratio ( $m/z$ ). Scan parameters included a resolution of 140.000, automatic gain control (AGC) target value of  $3e6$ , maximum injection time of 200 ms, capillary temperature of 275 °C, S-Lens RF factor of 70, and a sample tray temperature of 18 °C. Data acquisition was performed using Xcalibur software (version 3.0, Thermo Fisher Scientific). RAW files were converted to mzXML format using ThermoRawFileParser (version 1.1.11, Thermo Fisher Scientific). Next, mzXML files were processed using our customized bioinformatics pipeline, which annotates mean peak intensities of technical triplicates using the human metabolome database (Source code available at <https://github.com/UMCUGenetics/DIMS>, version 3.0).

### **Hemoglobin-oxygen affinity**

The affinity between hemoglobin molecules and oxygen was assessed via the Hemox Analyzer (TCS Scientific Corporation), which determines the hemoglobin-oxygen oxygen equilibrium curve (OEC) by calculating the percentage of oxyhemoglobin at a decreasing oxygen tension (from atmospheric pressure to 1.5 mmHg as the lowest pressure). The percentage of bound oxyhemoglobin is measured via dual-wave spectrophotometry at 560 nm (deoxyhemoglobin) and 576 nm (oxyhemoglobin), whilst the oxygen tension is measured via an oxygen-sensing electrode. The outcome parameter,  $p_{50}$ , is determined by calculating the oxygen tension at which 50% of measured hemoglobin is saturated with oxygen. For this measurement, 40  $\mu$ L of whole blood or *ex vivo* treated RBCs are diluted in 4 mL of Hemox buffer (containing 30 mM TES buffer (TES and TES sodium salt (both Sigma-Aldrich) and 5 mM KCl, osmolality adjusted to 293 mOsm/kg with NaCl, pH 7.41 at 37 °C) with additional BSA (0.08%) and anti-foam (0.02%).

## Ektacytometry

The laser-optical rotational red cell analyzer (Lorrca, RR Mechatronics) was used for ektacytometry analyses. During measurements, shear stress is imposed on the RBCs via to force from a rotating cylinder. The RBCs deform, and this deformation can be detected via a diffraction pattern produced by a laser and is expressed as the elongation index (EI). For all measurements, whole blood or *ex vivo* treated RBCs were diluted in ElonISO (viscosity 29.50 mPa·s, osmolality 283 mOsm/kg, pH 7.44, Boom) at various concentrations. Deformability curves were obtained by exposing RBCs (concentration in ElonISO  $60 \times 10^6$  RBCs/mL) to shear stresses between 0.3 Pa and 100 Pa and measuring the EI at nine different shear points. Parameters derived from the deformability assay were the  $EI_{max}$ . Osmotic gradient ektacytometry was performed by exposing RBCs (concentration in ElonISO  $200 \times 10^6$  RBCs/mL) to an osmotic gradient, starting at  $\pm 50$  mOsm/kg to a maximal osmolality of  $\pm 500$  mOsm/kg. The osmotic gradient was created by mixing OsmoLow (viscosity 30.40 mPa·s, osmolality 48 mOsm/kg) and OsmoHigh (viscosity 30.57 mPa·s, osmolality 671 mOsm/kg) (containing polyvinylpyrrolidone 360 and PBS (both Sigma-Aldrich), desired osmolality is reached by addition of NaCl). Parameters derived from the osmotic gradient ektacytometry were  $EI_{min}$  (minimum measured EI),  $O_{min}$  (osmolality at the  $EI_{min}$ , which is commonly increased in HS, reflecting the decreased surface area/volume ratio),  $EI_{max}$  (maximum measured EI, typically decreased in HS, reflecting the decreased membrane surface),  $O_{max}$  (osmolality at which  $EI_{max}$  is reached),  $O_{hyper}$  (osmolality corresponding to 50% of the  $EI_{max}$ , which may be decreased in HS, indicating dehydration of the RBCs), and the area under the curve (AUC, the area starting at  $O_{min}$  up to the measured point at 500 mOsm/kg). During the cell-membrane stability test (CMST), RBCs (concentration in ElonISO  $60 \times 10^6$  RBCs/mL) are exposed to a shear of 100 Pa for 30 minutes, after which the difference between the initial EI ( $EI_{max-CMST}$ ) and EI measured at the end of the 30 minutes ( $EI_{min-CMST}$ ) is determined (both  $EI_{max-CMST}$  and  $EI_{min-CMST}$  are calculated as the median from respectively the first ten and final ten measurement values). Due to the continuous shear stress, RBCs shed part of their membrane, leading to a decrease in EI. However, in HS, RBCs are less prone to membrane loss, most likely to the rigidity of the dense RBCs. It has been proposed that the CMST may reflect membrane health in spherocytosis, and thus could be used as a biomarker to evaluate treatment effects.

## Adhesion to laminin

Polymer  $\mu$ -slides (uncoated  $\mu$ -Slide I Luer 0.4 mm in height, Ibidi) were incubated with laminin (BioLamina) for two hours at 37 °C on the day of measurement. *Ex vivo* treated RBCs were diluted in a HEPES buffer (containing 132 mM NaCl, 6 mM KCl, 1 mM  $MgSO_4$ , 1.2 mM  $K_2HPO_4$ , 1 mM  $CaCl_2$ , 20 mM HEPES, 5.55 mM glucose and 0.5% BSA, pH 7.40) and were then brought under a pushing flow (0.5 dyne/cm<sup>2</sup>) through the laminin-coated microfluidic slide. After a continuous flow of RBCs for 10 minutes at room temperature, non-adherent cells were washed away by adding HEPES buffer without RBCs for two minutes under the same flow. In total,  $1.52 \times 10^8$  RBCs were brought under flow per condition. Nine brightfield photos were taken (using the Zeiss Observer Z1 microscope (20x objective)), and the number of adhered RBCs per photo was counted. The average number of adhered RBCs was calculated and used as outcome parameter.

### **Intracellular calcium quantification**

RBCs (concentration  $20 \times 10^6/\text{mL}$ ) were incubated for 1 hour at  $37^\circ\text{C}$  in a Tyrode buffer (containing 135 mM NaCl, 5.4 mM KCl, 1 mM  $\text{MgSO}_4$ , 1.8 mM  $\text{CaCl}_2$ , 10 mM HEPES and 10 mM Glucose, pH 7.40) with Fluo-4-AM (Invitrogen by Thermo Fisher Scientific,  $5\ \mu\text{M}$ ). After this incubation, the cells were washed and diluted in Tyrode buffer to a concentration of  $6.67 \times 10^6/\text{mL}$ . The stained cells were analyzed by flow cytometry (FACS Canto II, BD Biosciences). The mean fluorescent intensity of single RBCs (based on sideward and forward scatter) was measured via the FITC channel, in triplicate. Due to the known rapid changes in intracellular calcium levels, each condition was handled exactly in the same manner and with the same duration, to prevent the effect of time on mean fluorescent intensity outcomes.

### **Statistical analysis**

All data (except from the untargeted metabolomics) were analyzed via GraphPad Prism Version 10.2.3 (347). Gaussian distribution was determined via the Shapiro-Wilk test, which determined the test used for assessing differences between various groups. Appropriately, either the T-test, Welch T-test, One-Way ANOVA or Friedman test were performed. When certain values were missing, a mixed-effects analysis was additionally used to the One-Way ANOVA. Dunnett's multiple comparison test was used. To determine correlations, Spearman non-parametric testing was performed. As for the untargeted metabolomics, the annotated mass peak intensities were first converted to Z-scores, which were calculated by the following formula:

$$Z - score = \frac{(\text{Mass peak intensity of sample} - \text{Mean mass peak intensity of HC or vehicle samples})}{\text{Standard deviation mass peak intensities of HC or vehicle samples}}$$

The Z-scores were then analyzed in MetaboAnalyst (version 6.0), without any data filtering or normalization. The metabolic variation between samples was analyzed by the unsupervised principal component analysis (PCA) to reduce the dimensionality of the data and capture the largest variation between samples in a few principal components. The most significantly differing metabolites (between two groups, determined via *t*-tests) were displayed in heatmaps. The heatmaps were created without clustering of samples and with autoscaling of metabolites.

## SUPPLEMENTAL FIGURES.

### **Supplemental Figure 1 – Western blot analysis of pyruvate kinase isozymes R and M2 in untreated red blood cell lysates of hereditary spherocytosis patients.**

(A) Pyruvate kinase (PK) R, the red blood cell (RBC) specific PK isoform, was quantified using western blot analysis and related to actin, the loading control. RBC lysate from an identical healthy control (HC) was used in three different western blots, as an internal control. (B) An increased PKR/Actin ratio was significantly associated with an increase in reticulocyte percentage. Squared symbols represent the splenectomized patients. (C) Bands corresponding to PKR and Actin in the individual HS patients. (D) Western blot results for the PKM2 isoform. THP-1 cell lysate was used as a positive control here. HC healthy control; HS hereditary spherocytosis; PKM2 pyruvate kinase M2; PKR pyruvate kinase R.

### **Supplemental Figure 2 – Correlation between 2,3-diphosphoglycerate levels and p50 values in untreated whole blood of hereditary spherocytosis patients.**

A dot-plot showing the correlation between the measured 2,3-diphosphoglycerate (2,3-DPG) levels and the p50 values. Squared symbols represent the splenectomized patients. DPG diphosphoglycerate; RBC red blood cell.

### **Supplemental Figure 3 – Evaluating the effect of pyruvate kinase activation on pyruvate kinase thermostability.**

For this assay, lower concentrations of PK activators were used (mitapivat 2  $\mu$ M, tebapivat 2  $\mu$ M and 500 nM). Pyruvate kinase (PK) thermostability was measured at a phosphoenolpyruvate (PEP) concentration of 0.5 mM. (A-D) PK thermostability is usually assessed after exposing the red blood cell (RBC) lysate for 60 minutes to 53°C. Here, we show the PK thermostability after 5, 10, 20 and 40 minutes. These lysates were incubated with either vehicle or PK activator prior to the PK thermostability assay (N=17). DMSO dimethylsulfoxide; PK pyruvate kinase. Error bars represent standard deviation. \*\* $p < 0.01$ , \*\*\* $p < 0.001$ , \*\*\*\* $p < 0.0001$ , ns not significant.

### **Supplemental Figure 4 - Differences in metabolome of untreated whole blood between hereditary spherocytosis patients and healthy controls.**

(A) Principal component analysis (PCA) of whole blood samples from hereditary spherocytosis (HS) patients (red, N=18) and healthy controls (HC) (green, N=9) displayed with 95% confidence regions. Sample names are displayed, and each number corresponds to an individual sample. (B) Heatmap of the 50 most significantly different metabolites between HCs and HS patients as identified by unpaired t-tests (unadjusted  $p < 0.01$ ). Among the top 50 significantly different metabolites were several polyamines and carnitines. A comprehensive overview of  $p$ -values and isomers is displayed in Supplemental File 1.

HC healthy control; HS hereditary spherocytosis; PC principal component.

### **Supplemental Figure 5 – Correlations between decreases in 2,3-diphosphoglycerate and p50.**

(A) The p50 values expressed in mmHg of the differently treated RBCs (vehicle, mitapivat 10  $\mu$ M, tebapivat 10  $\mu$ M, and tebapivat 2  $\mu$ M). (B-D) The decreases in p50 value and 2,3-

diphosphoglycerate (2,3-DPG) upon *ex vivo* treatment with both pyruvate kinase (PK) activators were compared to each other, to determine whether there is a positive correlation between these decreases. In none of the conditions this resulted in a positive correlation (N=13).

DMSO dimethylsulfoxide; DPG diphosphoglycerate.

**Supplemental Figure 6 - Evaluation of osmotic gradient ektacytometry outcomes upon *ex vivo* treatment with mitapivat and tebapivat.**

(A-C) Changes in  $O_{min}$ ,  $O_{max}$  and AUC upon PK activation are shown (N=14 for  $O_{min}$  and AUC, N=15 for  $O_{max}$ ). (D) A representative osmotic gradient ektacytometry graph is depicted, including the curves of the treated red blood cells (RBCs). The various osmotic gradient ektacytometry parameters are noted.

DMSO dimethylsulfoxide; EI elongation index. Error bars represent standard deviation. \* $p < 0.05$ , \*\* $p < 0.01$ , ns not significant.

**Supplemental Figure 7 – Effects of *ex vivo* pyruvate kinase activation on the deformability assay and cell membrane stability test.**

(A) Results of *ex vivo* treatment with both PK activators on the  $EI_{max}$  as determined by the deformability assay (shear stress 0.3-100 Pa) (N=10). (B) The results of the cell membrane stability test (CMST), in which hereditary spherocytosis (HS) red blood cells (RBCs) have a decreased  $\Delta EI$  due to their incapability of shedding membrane, upon *ex vivo* treatment are shown (N=12).

DMSO dimethylsulfoxide; EI elongation index. Error bars represent standard deviation. ns not significant.

**Supplemental Figure 8 – Comparison of different disease severities in terms of metabolism and response to *ex vivo* pyruvate kinase activation.**

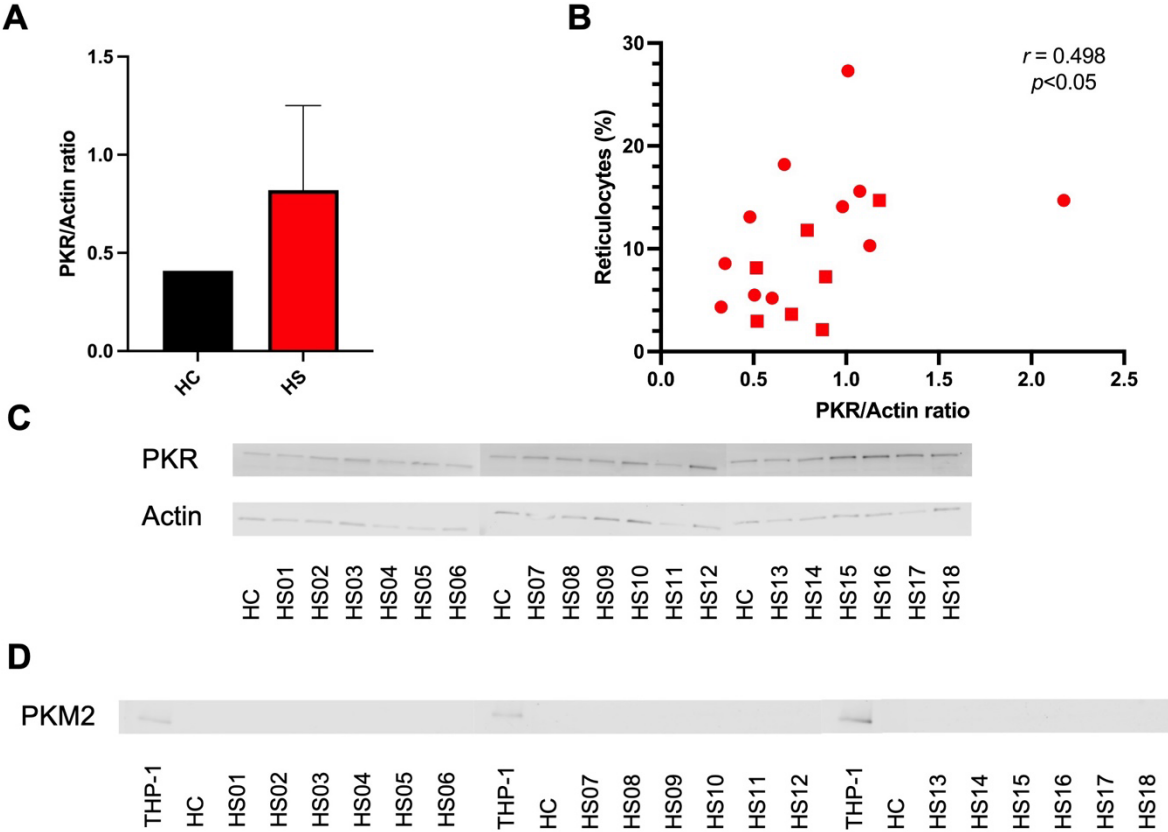
(A-C) Hereditary spherocytosis (HS) patients were categorized as mild, moderate or severe according to hemoglobin level and reticulocyte percentage. Differences in pyruvate kinase/hexokinase (PK/HK) ratio, PK thermostability and adenosine triphosphate/2,3-diphosphoglycerate ratio. (D-E) Response to *ex vivo* PK activation was compared between the disease severities, in all three treatment conditions (mitapivat 10  $\mu M$ , tebapivat 10  $\mu M$  and tebapivat 2  $\mu M$ ). For PK thermostability, phosphoenolpyruvate (PEP) 0.5 mM final concentration was used.

ATP adenosine triphosphate; DMSO dimethylsulfoxide; DPG diphosphoglycerate; HK hexokinase; PK pyruvate kinase. Median is shown; error bars represent interquartile ranges.

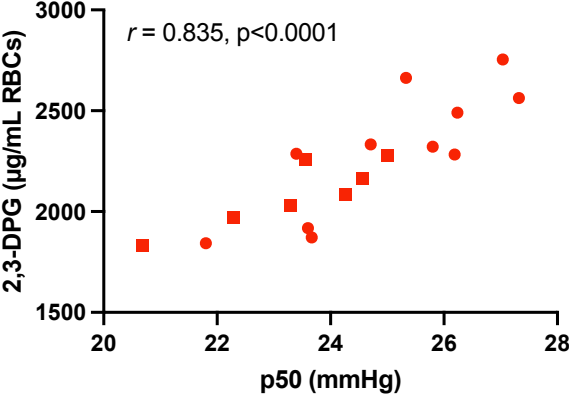
**Supplemental File 1** – Excel sheet containing all significantly different metabolites between untreated whole blood of patients with hereditary spherocytosis and healthy controls.

**Supplemental File 2** - Excel sheet containing all significantly different metabolites between the hereditary spherocytosis red blood cells treated with vehicle and those treated with tebapivat 2  $\mu M$ .

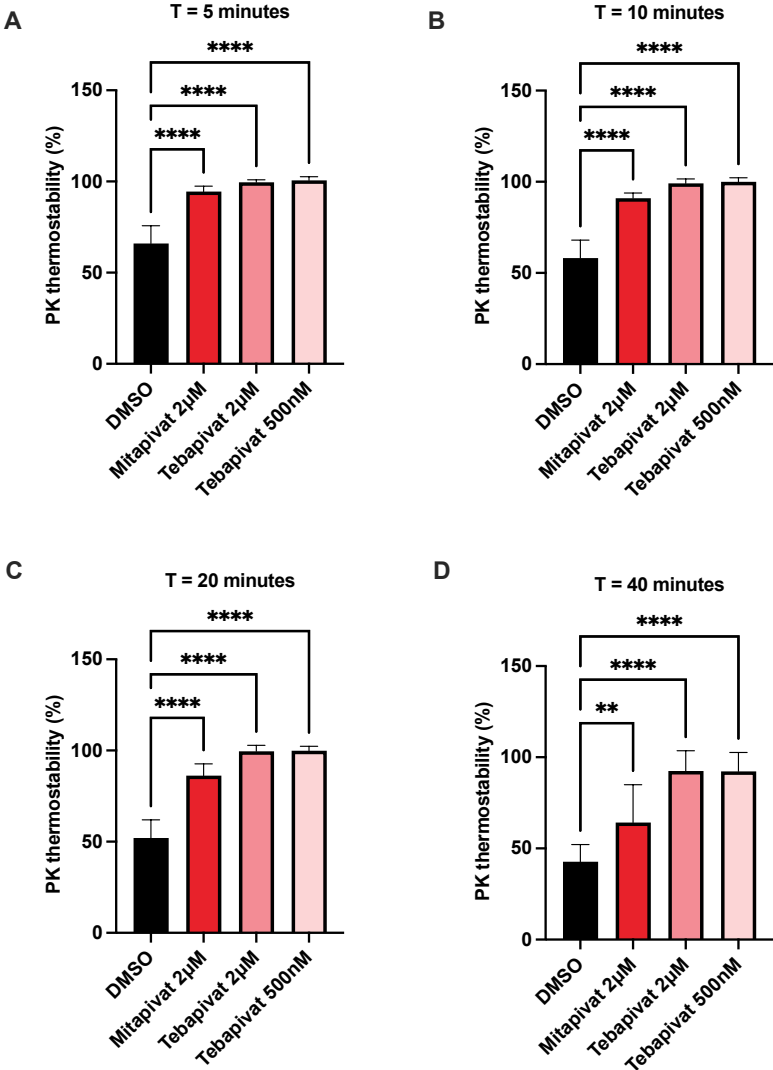
**Supplemental Figure 1 – Western blot analysis of pyruvate kinase isozymes R and M2 in untreated red blood cell lysates of hereditary spherocytosis patients.**



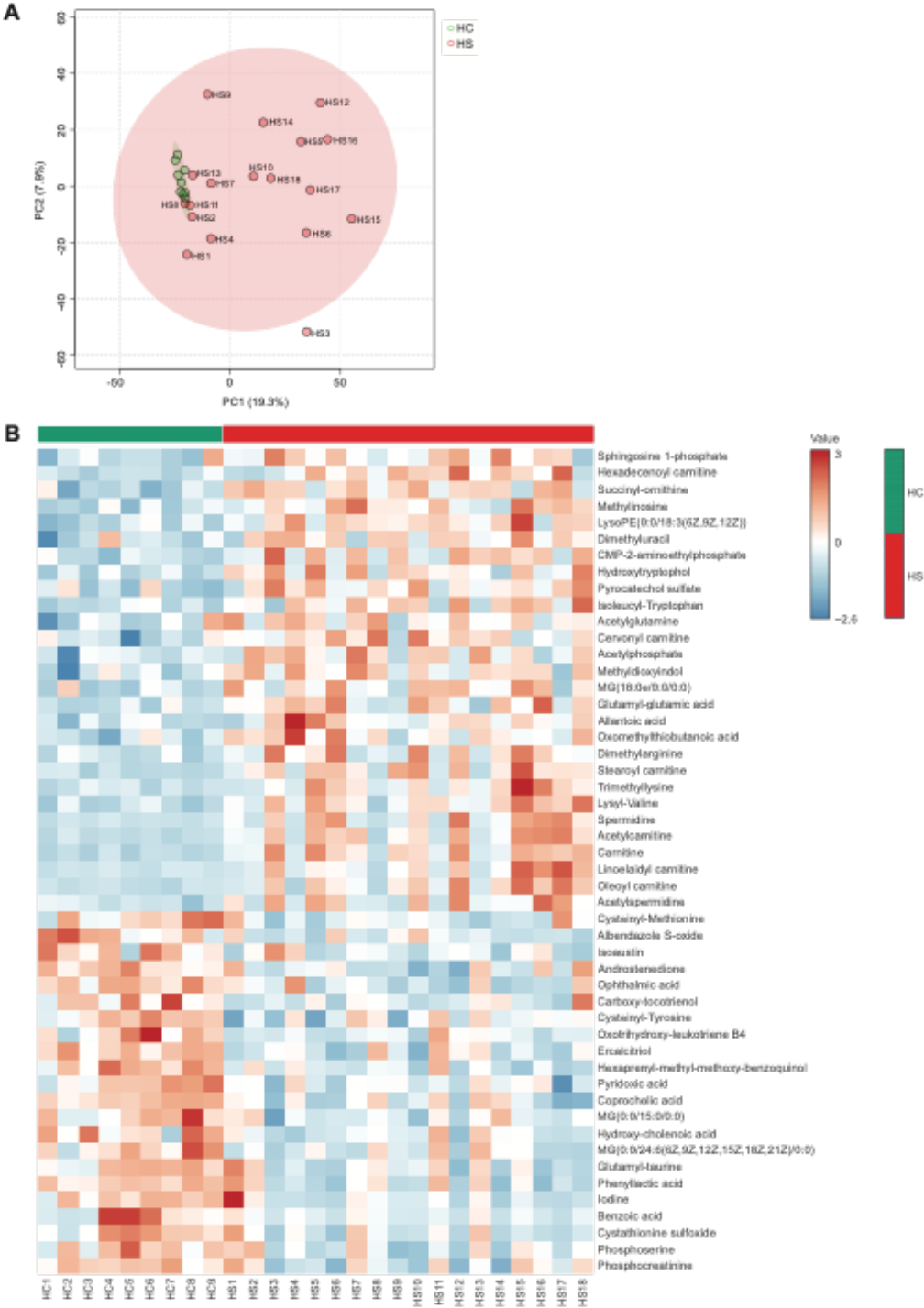
**Supplemental Figure 2 – Correlation between 2,3-diphosphoglycerate levels and p50 values in untreated whole blood of hereditary spherocytosis patients.**



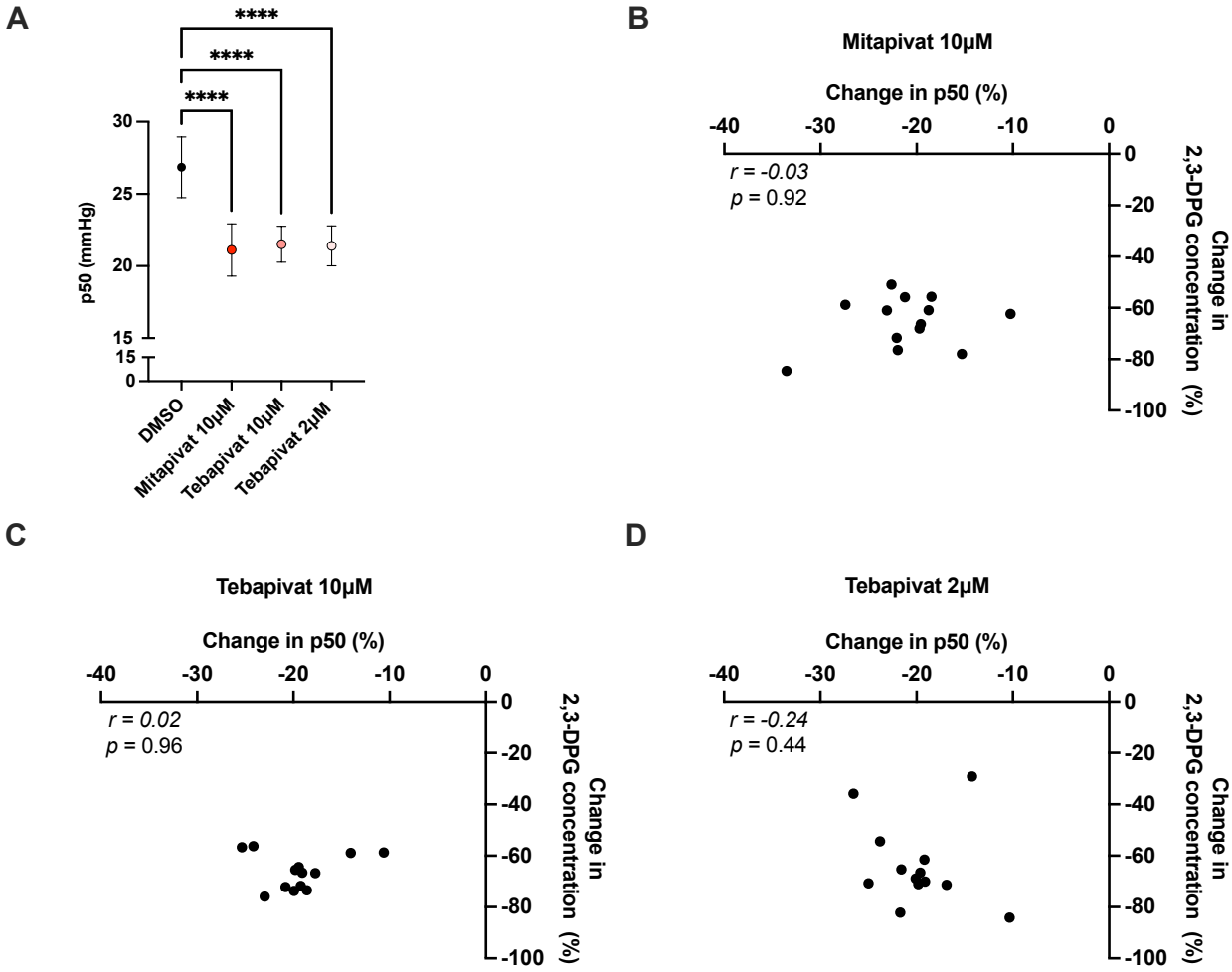
**Supplemental Figure 3 – Evaluating the effect of pyruvate kinase activation on pyruvate kinase thermostability.**



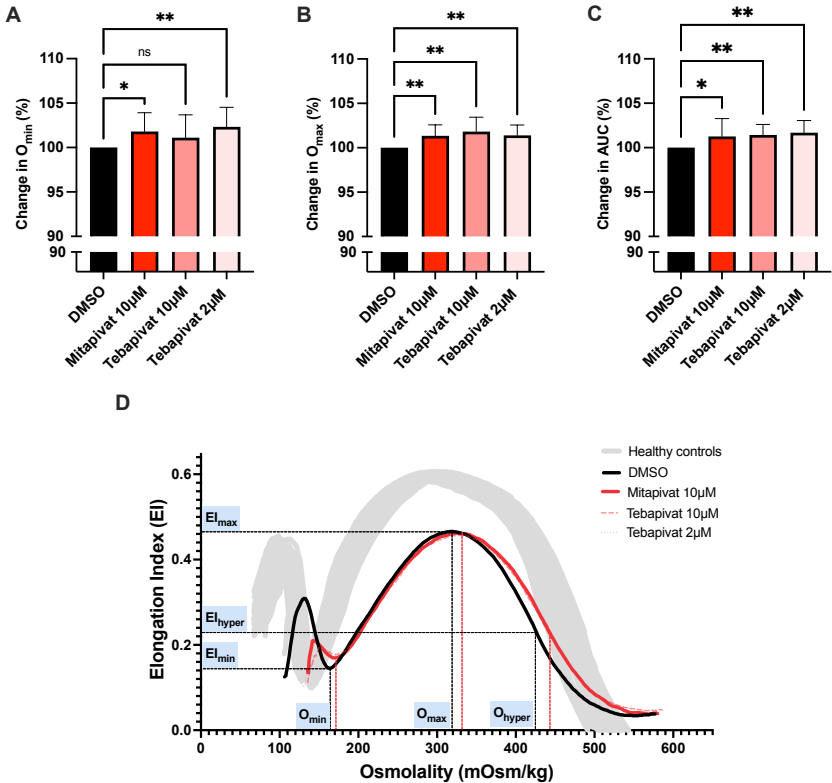
**Supplemental Figure 4 – Differences in metabolome of untreated whole blood between hereditary spherocytosis patients and healthy controls.**



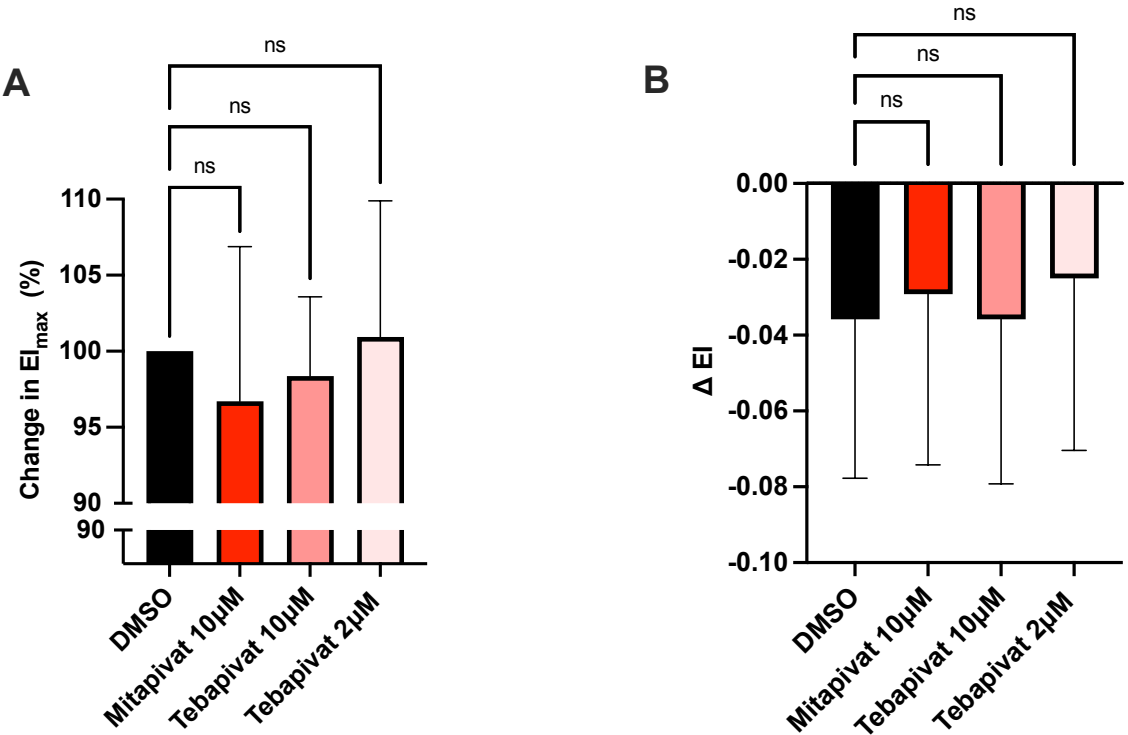
**Supplemental Figure 5 – Correlations between decreases in 2,3-diphosphoglycerate and p50.**



**Supplemental Figure 6 – Evaluation of osmotic gradient ektacytometry outcomes upon *ex vivo* treatment with mitapivat and tebapivat.**



Supplemental Figure 7 – Effects of *ex vivo* pyruvate kinase activation on the deformability assay and cell membrane stability test.



**Supplemental Figure 8 - Comparison of different disease severities in terms of metabolism and response to ex vivo pyruvate kinase activation.**

